INTERNATIONAL JOURNAL FOR NUMERICAL METHODS IN ENGINEERING
Int. J. Numer. Meth. Engng 2010; **82**:205–241
Published online 15 October 2009 in Wiley InterScience (www.interscience.wiley.com). DOI: 10.1002/nme.2753

Energy-stepping integrators in Lagrangian mechanics

M. Gonzalez[1], B. Schmidt[2] and M. Ortiz[1,*,†]

[1]*Graduate Aeronautical Laboratories, California Institute of Technology, Pasadena, CA 91125, U.S.A.*
[2]*Zentrum Mathematik, Technische Universität München, Boltzmannstr. 3, 85747 Garching, Germany*

SUMMARY

We present a class of integration schemes for Lagrangian mechanics, referred to as *energy-stepping integrators*, that are momentum and energy conserving, symplectic and convergent. In order to achieve these properties we replace the original potential energy by a piecewise constant, or *terraced* approximation at steps of uniform height. By taking steps of diminishing height, an approximating sequence of energies is generated. The trajectories of the resulting approximating Lagrangians can be characterized explicitly and consist of intervals of piecewise rectilinear motion. We show that the energy-stepping trajectories are symplectic, exactly conserve all the momentum maps of the original system and, subject to a transversality condition, converge to trajectories of the original system when the energy step is decreased to zero. These properties, the excellent long-term behavior of energy-stepping and its automatic time-step selection property, are born out by selected examples of application, including the dynamics of a frozen Argon cluster, the spinning of an elastic cube and the collision of two elastic spheres. Copyright © 2009 John Wiley & Sons, Ltd.

Received 26 March 2009; Revised 21 August 2009; Accepted 24 August 2009

KEY WORDS: Lagrangian mechanics; time-integration; symplectic integrators; energy-momentum integrators

1. INTRODUCTION

The formulation of convergent time-integration schemes with exact conservation properties has been a longstanding goal of numerical analysis and computational mechanics. In a seminal contribution, Ge and Marsden [1] showed that, in general, integrators with a fixed time step cannot simultaneously preserve energy, the symplectic structure and other conserved quantities, such as linear and angular momenta. This observation led to a dichotomy in the literature between symplectic-momentum and energy-momentum integrators. In principle, symplectic-energy-momentum integrators can be devised by adopting a space-time viewpoint and allowing for time-step adaption in order to

*Correspondence to: M. Ortiz, Graduate Aeronautical Laboratories, California Institute of Technology, Pasadena, CA 91125, U.S.A.
†E-mail: ortiz@aero.caltech.edu

satisfy the constraint of conservation of energy [2]. However, due to lack of solvability of the time-step optimization problem, especially near *turning points* where velocities are small [2, 3], non-energy-preserving steps are inevitable in some schemes.

The design of symplectic-momentum methods can be accomplished in a systematic and natural manner by recourse to a discrete version of Hamilton's variational principle (cf., for example [4–6]; see also [7], Chapter VIII, and references therein) based on an approximating discrete Lagrangian. The resulting variational time integrators are, for a nondissipative and nonforced case, symplectic and momentum preserving. However, it should be carefully noted that the momenta conserved by variational integrators are those corresponding to the discrete Lagrangian, which in general approximate—but differ from—those of the original Lagrangian. Many standard integrators, whether explicit or implicit, are indeed variational in this sense, including the widely used Newmark method [8], midpoint rule, symplectic partitioned Runge–Kutta schemes, and others (cf., for example Marsden and West [4] for details). Experience has shown that, while not being exactly energy conserving, constant time-step symplectic-momentum methods tend to exhibit a good energy behavior over long times (see, for example, [8] and references therein), though the good energy behavior tends to degrade when variable time steps are used [9, 10].

In general, good geometrical and invariance properties do not supply a guarantee of good accuracy and convergence of integration schemes, which must be carefully analyzed separately. In the context of linear structural systems, a powerful tool for investigating convergence is furnished by *phase-error analysis* [11–13]. Phase-error analysis aims to establish the convergence of the amplitude and frequency of oscillatory numerical solutions to the amplitude and frequency of the exact solution. Phase-error analysis is a particularly powerful tool inasmuch as it establishes the convergence of solutions in a global, instead of merely local, sense. This attribute is in analogy to backward error analysis [7, 14, 15], which is also global in nature, and in contrast to other conventional methods of analysis, such as Gronwall's inequality [4], which provide local exponential bounds on discretization errors. The engineering literature on the subject of phase-error analysis relies on a case-by-case analysis of linear time-stepping algorithms. An extension of phase-error analysis to nonlinear systems may be accomplished by recourse to notions of Γ-convergence [16].

The work presented in this paper is concerned with the formulation of time-integration schemes for Lagrangian mechanics that are symplectic and exactly conserve all the invariants of the system by construction. We achieve these desirable properties by the simple device of replacing the potential energy of the system by an approximating sequence of energies that have the same invariance properties as the original potential energy and whose trajectories can be characterized exactly. This strategy may be regarded as the reverse of that underlying backward-error analysis. Thus, whereas backward-error analysis seeks to identify a nearby Lagrangian that is solved exactly by the solutions generated by a numerical integrator, the approach followed here is to directly replace the Lagrangian by a nearby one that can be solved exactly. If the approximating Lagrangians are constructed so as to have the same symmetries as the original Lagrangian, then it follows from standard theory that all the invariants, or momentum maps, of the original system are conserved exactly by the numerical solutions. Additionally, as the numerical trajectories are exact solutions of a Lagrangian, it follows that the numerical trajectories are symplectic. By generating a sequence of approximating Lagrangians that converges to the original Lagrangian in an appropriate sense, a sequence of approximating trajectories is generated, which may be expected to converge to trajectories of the original system. By this simple procedure, momentum and energy conserving, symplectic and convergent time-integration schemes can be constructed.

DOI: 10.1002/nme

We specifically investigate piecewise-constant approximations of the potential energy. Thus, we replace the original potential energy by a stepwise, or *terraced*, approximation at steps of uniform height. By taking energy steps of diminishing height, an approximating sequence of energies is generated. The solutions of the approximating Lagrangians thus defined are piecewise rectilinear and can be constructed explicitly. In reference to the manner in which the potential energy is approximated and the numerical solution proceeds, we refer to the resulting integration scheme as *energy-stepping*. The rectilinear segments that comprise the energy-stepping trajectory span constant-energy surfaces and are thus of variable duration, which results in automatic time-step selection. By construction, the approximating Lagrangians are invariant under all the action groups that the original Lagrangian is itself invariant under, that is the approximating Lagrangians inherit all the symmetries of the original Lagrangian, and thus the energy-stepping solution conserves all the momentum maps of the original Lagrangian exactly. In addition, as the energy-stepping trajectories are exact solutions of a Lagrangian, they are automatically symplectic. Furthermore, we show that, subject to a technical transversality condition, the energy-stepping trajectories converge to trajectories of the original system as the energy step decreases to zero.

The paper is organized as follows. The energy-stepping time-integration scheme is defined in Section 2. The conservation properties of energy-stepping are presented in Section 3. In Section 4 we proof convergence of trajectories satisfying a transversality condition. Finally, in Section 5 we present selected examples of application that illustrate the convergence, accuracy and conservation properties of energy-stepping, including the dynamics of a frozen Argon cluster, the spinning of an elastic cube and the collision of two elastic spheres. Finally, a summary and concluding remarks are collected in Section 6.

2. ENERGY-STEPPING INTEGRATORS

For definiteness, we specifically consider dynamical systems characterized by Lagrangians $L:\mathbb{R}^N\times\mathbb{R}^N\to\mathbb{R}$ of the form

$$L(q,\dot{q})=\tfrac{1}{2}\dot{q}^T M\dot{q}-V(q) \tag{1}$$

where M is the mass matrix and V is the potential energy. Lagrangians of this form arise in a number of areas of application including structural dynamics and molecular dynamics. The trajectories of a Lagrangian system can be approximated by replacing $L(q,\dot{q})$ by an approximating Lagrangian $L_h(q,\dot{q})$ that can be solved exactly. A particular type of approximating Lagrangian is

$$L_h(q,\dot{q})=\tfrac{1}{2}\dot{q}^T M\dot{q}-V_h(q) \tag{2}$$

obtained by introducing an approximation of the potential energy. In this work, we specifically investigate piecewise-constant approximations of the potential energy. Thus, we replace the original potential energy V by a stepwise or *terraced* approximation V_h at steps of uniform height h, namely,

$$V_h=\text{largest piecewise-constant function with values in } h\mathbb{Z} \text{ majorized by } V \tag{3}$$

or, equivalently,

$$V_h(q)=h\lfloor h^{-1}V(q)\rfloor \tag{4}$$

DOI: 10.1002/nme

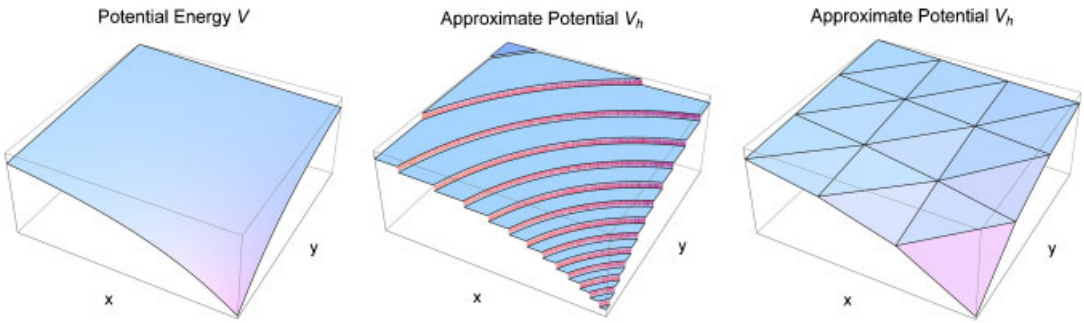

Figure 1. Kepler problem. Exact, piecewise constant and piecewise linear continuous approximate potential energies.

where $\lfloor\cdot\rfloor$ is the floor function, that is $\lfloor x\rfloor=\max\{n\in\mathbb{Z}:n\leqslant x\}$. By taking steps of diminishing height, an approximating sequence of potential energies and Lagrangians is generated in this manner. The chief characteristics of the new systems thus obtained are that they can be solved exactly, as demonstrated in Section 2.1, and that they have the same symmetries as the original system, as shown in Section 3. Evidently, other types of approximations, such as piecewise linear interpolations of the potential energy, also result in exactly integrable approximating systems. However, a naive piecewise linear approximation breaks the symmetries of the system in general. Piecewise constant and piecewise linear approximations of the Kepler potential are shown in Figure 1 by way of illustration.

2.1. Computation of the exact trajectories of the approximating Lagrangian

We now proceed to compute the exact trajectories of the approximate Lagrangian $L_h(q,\dot{q})$ resulting from the piecewise-constant approximation (3) of the potential energy. Suppose that the system is in configuration q_0 at time t_0 and in configuration q_2 at time t_2 and that during the time interval $[t_0,t_2]$ the system intersects one single jump surface Γ_1 separating two regions of constant energies V_0 and V_2, Figure 2. By the construction of V_h, Γ_1 is the level surface $V=V_2$ for an uphill step $V_2=V_0+h$, or the level surface $V=V_0$ for a downhill step $V_2=V_0-h$. For simplicity, we shall further assume that V is differentiable and that all energy-level crossings are transversal, that is

$$n(q_1)\cdot\dot{q}_1^-\neq 0 \tag{5}$$

where $\dot{q}_1^-=\dot{q}(t_1^-)$ and $n(q_1)$ is a vector normal to Γ_1 pointing in the direction of advance.

It is possible for discrete trajectories be *trapped* and become *embedded* within a jump surface for a finite time interval, for example when the intersection of the trajectory with the jump surface is non transversal and the surface turns toward the trajectory in the direction of advance. In this case, the embedded trajectory segment is a geodesic of the jump surface in metric defined by the mass matrix M. However, the likelihood of non transversal intersections resulting in the trapping of trajectories within jump surfaces is exceedingly low in practical applications and will not be given further consideration.

DOI: 10.1002/nme

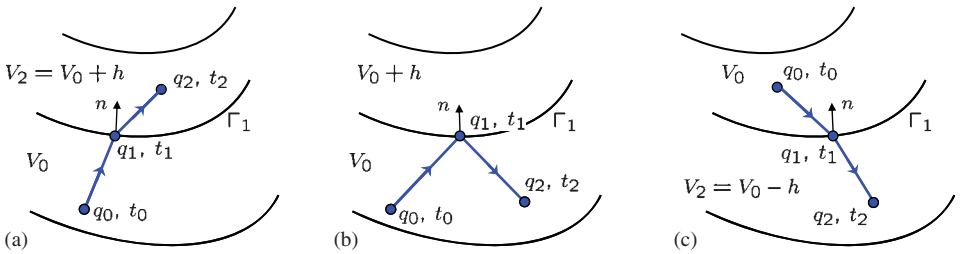

Figure 2. Trajectory of a system whose potential energy is approximated as piecewise constant: (a) positive step; (b) reflection; and (c) negative step.

Under the preceding assumptions, the action integral over the time interval $[t_0, t_2]$ follows as:

$$I_h = \int_{t_0}^{t_2} L_h(q,\dot{q})\,\mathrm{d}t = \int_{t_0}^{t_1} L_h(q,\dot{q})\,\mathrm{d}t + \int_{t_1}^{t_2} L_h(q,\dot{q})\,\mathrm{d}t \tag{6}$$

where t_1 is the time at which the trajectory intersects Γ_1. In regions where $V_h(q)$ is constant the trajectory $q(t)$ is linear in time. Therefore, the action of the system can be computed exactly and reduces to

$$I_h = (t_1 - t_0)\left\{\frac{1}{2}\left(\frac{q_1 - q_0}{t_1 - t_0}\right)^{\mathrm{T}} M \left(\frac{q_1 - q_0}{t_1 - t_0}\right) - V_0\right\} + (t_2 - t_1)\left\{\frac{1}{2}\left(\frac{q_2 - q_1}{t_2 - t_1}\right)^{\mathrm{T}} M \left(\frac{q_2 - q_1}{t_2 - t_1}\right) - V_2\right\} \tag{7}$$

where $q_1 = q(t_1)$ is constrained to be on the jump surface Γ_1. Assuming differentiability of Γ_1, stationarity of the action with respect to (t_1, q_1) additionally gives the energy conservation equation

$$\left(\frac{q_1 - q_0}{t_1 - t_0}\right)^{\mathrm{T}} M \left(\frac{q_1 - q_0}{t_1 - t_0}\right) + 2V_0 = \left(\frac{q_2 - q_1}{t_2 - t_1}\right)^{\mathrm{T}} M \left(\frac{q_2 - q_1}{t_2 - t_1}\right) + 2V_2 \tag{8}$$

and the linear momentum balance equation

$$M\frac{q_1 - q_0}{t_1 - t_0} - M\frac{q_2 - q_1}{t_2 - t_1} + \lambda n(q_1) = 0 \tag{9}$$

where λ is a Lagrange multiplier.

In order to make a more direct connection with time-integration schemes we reformulate the problem slightly by assuming that t_0, q_0—the latter on a jump surface Γ_0 except, possibly, at the initial time—and the initial velocity

$$\dot{q}_0^+ = \dot{q}(t_0^+) = \frac{q_1 - q_0}{t_1 - t_0} \tag{10}$$

are known. Let t_1 and q_1 be the time and point at which the trajectory intersects the next jump surface Γ_1. We then seek to determine

$$\dot{q}_1^+ = \dot{q}(t_1^+) \tag{11}$$

DOI: 10.1002/nme

A reformulation of Equations (8) and (9) in terms of $\dot{q}_1^+$ gives

$$(\dot{q}_1^+)^{\mathrm{T}} M \dot{q}_1^+ = (\dot{q}_1^-)^{\mathrm{T}} M \dot{q}_1^- - 2\Delta V \tag{12}$$

$$\dot{q}_1^+ = \dot{q}_1^- + \lambda M^{-1} n(q_1) \tag{13}$$

where $\dot{q}_1^- = \dot{q}_0^+$ and the energy jump $\Delta V = V_h(q(t_1^+)) - V_h(q(t_1^-))$. Next we proceed to parse through the various cases that arise in the solution of (12) and (13).

2.1.1. Diffraction by downhill energy step. Suppose that $\Delta V = -h$, that is the system decreases its energy as the trajectory crosses Γ_1. Then (12) becomes

$$(\dot{q}_1^+)^T M \dot{q}_1^+ = (\dot{q}_1^-)^T M \dot{q}_1^- + 2h \tag{14}$$

Then, the system (13)–(14) has the real solution

$$\dot{q}_1^+ = \dot{q}_1^- - \frac{\dot{q}_1^- \cdot n_1 + \sqrt{(\dot{q}_1^- \cdot n_1)^2 + 2h n_1^T M^{-1} n_1}}{n_1^T M^{-1} n_1} M^{-1} n_1 \tag{15}$$

This solution represents the diffraction, or change of direction, of the trajectory by a downhill energy step.

2.1.2. Diffraction by uphill energy step. Suppose now that $\Delta V = h$, that is the system increases its energy as the trajectory crosses Γ_1. Then (12) becomes

$$(\dot{q}_1^+)^{\mathrm{T}} M \dot{q}_1^+ = (\dot{q}_1^-)^{\mathrm{T}} M \dot{q}_1^- - 2h \tag{16}$$

Suppose, in addition, that

$$(\dot{q}_1^- \cdot n_1)^2 > 2h n_1^{\mathrm{T}} M^{-1} n_1 \tag{17}$$

Then, the system (13)–(16) again has a real solution, namely,

$$\dot{q}_1^+ = \dot{q}_1^- - \frac{\dot{q}_1^- \cdot n_1 + \sqrt{(\dot{q}_1^- \cdot n_1)^2 - 2h n_1^{\mathrm{T}} M^{-1} n_1}}{n_1^{\mathrm{T}} M^{-1} n_1} M^{-1} n_1 \tag{18}$$

This solution again represents the diffraction of the trajectory by an uphill energy step when the system has sufficient initial energy to overcome the energy barrier.

2.1.3. Reflection by uphill energy step. Suppose now that $\Delta V = h$, that is the system increases its energy as the trajectory crosses Γ_1, but, contrary to the preceding case,

$$(\dot{q}_1^- \cdot n_1)^2 < 2h n_1^{\mathrm{T}} M^{-1} n_1 \tag{19}$$

Then, the system (13)–(16) has no real solutions, showing that the system does not have sufficient initial energy to overcome the energy barrier. Instead, the trajectory remains within the same energy level and Equation (12) becomes

$$(\dot{q}_1^+)^{\mathrm{T}} M \dot{q}_1^+ = (\dot{q}_1^-)^{\mathrm{T}} M \dot{q}_1^- \tag{20}$$

DOI: 10.1002/nme

Then, the system (13)–(20) is solved by

$$\dot{q}_1^+ = \dot{q}_1^- - 2\frac{\dot{q}_1^- \cdot n_1}{n_1^{\mathrm{T}} M^{-1} n_1} M^{-1} n_1 \tag{21}$$

This solution represents the reflection of the trajectory by an uphill energy step when the system does not have sufficient initial energy to overcome the energy barrier.

2.2. Derivation of the Hamilton principle for the discontinuous energy-stepping potential by regularization

The energy-stepping potential (4) is not continuous and the corresponding action functional (6) is not Gateaux-differentiable on the space of curves in phase space. In particular, the first variation of I_h is not well-defined on this space and so the notion of critical points does not have a well-defined meaning in the classical sense. However, the calculations in the previous subsection can be given a rigorous interpretation by recourse to a smooth approximation procedure. In the spirit of identifying solutions to non smooth differential equations by suitable selection principles, we will show that the energy-stepping dynamics for fixed h is given by those solutions to (8) and (9) that are limiting trajectories of a nearby smooth dynamical system. It should be carefully noted that there are solutions to these equations other than those described in Section 2.1, as exemplified by a particle bouncing at an energy barrier that can be overcome energetically.

This approximation result has three important consequences:

(i) The notion of a critical point of I_h is given a rigorous definition.
(ii) The physical solutions to (8) and (9) are selected.
(iii) The existence of a nearby smooth system will prove extremely useful when investigating analytical aspects of the energy-stepping trajectories such as conservation properties (cf. Section 3).

Here, we call a solution q to Equations (8) and (9) *physical* if and only if q behaves as described in Sections 2.1.1, 2.1.2 or 2.1.3. For later use we note that this is the case if and only if q passes an energy jump surface precisely if this is possible without violating energy conservation. As a consequence, an energy-stepping trajectory is uniquely given by $q(0)$ and $\dot{q}(0)$.

For fixed $h>0$ consider the smooth approximation χ_ε to the stepping function $t \mapsto h\lfloor h^{-1}t \rfloor$ as given by the convolution

$$\chi(t) = \int_{\mathbb{R}} \varepsilon^{-1}\eta(\varepsilon^{-1}(t-s))h\lfloor h^{-1}s \rfloor \,\mathrm{d}s, \quad \varepsilon \ll h$$

where η denotes a standard mollifier, that is $\eta \in C_c^\infty(-1,1)$, $\eta \geqslant 0$ and $\int_{-1}^{1} \eta = 1$. Now define

$$L_{h,\varepsilon}(q,\dot{q}) = \tfrac{1}{2}\dot{q}^T M \dot{q} - V_{h,\varepsilon}(q) \quad \text{for } V_{h,\varepsilon}(q) := \chi_\varepsilon(V(q)) \tag{22}$$

As $L_{h,\varepsilon}$ is a smooth function, there is a well-defined classical dynamics corresponding to this Lagrangian. We will prove that, as $\varepsilon \to 0$, the critical points of the action functional

$$I_{h,\varepsilon}(q) = \int_{t_0}^{t_2} L_{h,\varepsilon}(q,\dot{q})\,\mathrm{d}t$$

converge to the trajectories identified in Section 2.

DOI: 10.1002/nme

More precisely, we have the following

Theorem 2.1
Suppose q is an energy-stepping trajectory satisfying $\nabla V(q)\neq 0$ and $(n\cdot\dot{q}^-)^2\notin\{0, 2hn^{\mathrm{T}}M^{-1}n\}$ for $n=n(q)=\nabla V(q)/|\nabla V(q)|$ on every energy jump surface. Let q_ε be the smooth trajectory corresponding to $L_{h,\varepsilon}$ with the same initial conditions $(q_0,\dot{q}_0)$. Then q_ε converges to q strongly in $W^{1,p}(0,T)$ for each $T>0$ and all $p<\infty$ and weak* in $W^{1,\infty}(0,T)$. Moreover, $\dot{q}_\varepsilon\to\dot{q}$ uniformly on $[0,T]\setminus S_r(q)$ for every $r>0$, where $S_r(q)$ is the r-neighborhood of the jump set of $\dot{q}$.

It is worth noting that a proof for this result can be given that does not make use of the explicit formulae for q obtained in Section 2. Instead, we will see that limiting trajectories satisfy the discrete variational principle leading to (8) and (9) and thus give an *a priori* justification of the procedure employed in Section 2 to compute q.

Proof
First note that as $\varepsilon\to 0$, $\chi_\varepsilon(V(q))\to h\lfloor h^{-1}V(q)\rfloor=V_h(q)$. In particular, $q_\varepsilon(t)$ is linear in time except in a small neighborhood of the energy jump surfaces. It suffices to consider the case when q meets a jump surface Γ precisely once, at time $t_1\in(t_0,t_2)$, say, and so we may assume that q is a physical solution to (8) and (9).

We begin by showing that $q_\varepsilon\to\tilde{q}$ as $\varepsilon\to 0$ strongly in $W^{1,p}(t_0,t_2)$ for all $p<\infty$ (and weak* in $W^{1,\infty}(t_0,t_2)$), where $\tilde{q}$ is linear on (t_0,t_1) and (t_1,t_2). By Γ_ε we denote the neighborhood of Γ defined by

$$\Gamma_\varepsilon=\{x\in\mathbb{R}^N : V_2-\varepsilon\leqslant V(x)\leqslant V_2+\varepsilon\}$$

Note that as $\nabla V(q(t_1))\neq 0$ by assumption, in the vicinity of $q(t_1)$, Γ_ε lies in an $O(\varepsilon)$-neighborhood of Γ. q_ε being a critical point of $I_{h,\varepsilon}$ satisfies the Euler–Lagrange equation

$$\ddot{q}_\varepsilon=-M^{-1}\nabla V_{h,\varepsilon}$$

Choose $\tau_{1,\varepsilon}$, $\tau_{2,\varepsilon}$ such that q_ε enters Γ_ε at time $t_1-\tau_{1,\varepsilon}$ and leaves it at time $t_1+\tau_{2,\varepsilon}$. Writing

$$\nabla V_{h,\varepsilon}(x)=\alpha(x)n+\beta(x)Px$$

for $n=n(q(t_1))$, P the projection onto the plane perpendicular to n and α, $\beta\in\mathbb{R}$, we obtain that $|\beta(x)|$ is bounded on $r\varepsilon$-neighborhoods of $q(t_1)$ independently of ε for each $r\in\mathbb{R}$, whereas $\alpha(x)$ scales with ε^{-1}. Splitting the trajectories accordingly as

$$q_\varepsilon(t)=q_\varepsilon^{\parallel}(t)+q_\varepsilon^{\perp}(t)\quad\text{with } q_\varepsilon^{\parallel}\in q(t_1)+\mathbb{R}M^{-1}n,\, q_\varepsilon^{\perp}\in M^{-1}P\mathbb{R}^N \tag{23}$$

we obtain that

$$\ddot{q}_\varepsilon^{\parallel}(t)=-M^{-1}\alpha(q_\varepsilon(t))n,\quad \ddot{q}_\varepsilon^{\perp}(t)=-M^{-1}\beta(q_\varepsilon(t))Pq_\varepsilon(t)$$

It is not hard to see that $\tau_{2,\varepsilon}+\tau_{1,\varepsilon}=O(\varepsilon)$ and so

$$|\ddot{q}_\varepsilon^{\parallel}(t)+M^{-1}\alpha(q_\varepsilon^{\parallel}(t))n|,\ |\ddot{q}_\varepsilon^{\perp}(t)|\leqslant C$$

on $(t_1-\tau_{1,\varepsilon},t_1+\tau_{2,\varepsilon})$ for some suitable constant $C>0$. This proves that in fact $\dot{q}_\varepsilon^{\perp}(t_1-\tau_{2,\varepsilon})-\dot{q}_\varepsilon^{\perp}(t_1-\tau_{1,\varepsilon})\to 0$ as $\varepsilon\to 0$ and, by energy conservation,

$$\dot{q}_\varepsilon(t_1-\tau_{2,\varepsilon})-\dot{q}_\varepsilon(t_1-\tau_{1,\varepsilon})\to\dot{q}^+-\dot{q}^-$$

DOI: 10.1002/nme

where $\dot{q}^+$ is given by (15) resp. (18) resp. (21). From here it is now straightforward to obtain that q_ε converges to $\tilde{q}$, where $\tilde{q}$ is linear on (t_0, t_1) and (t_1, t_2) and satisfies the jump condition (15) resp. (18) resp. (21) at t_1.

As we do not wish to use the fact that q is explicitly given by these equations in our proof, we proceed as follows. As q_ε is a critical point of $I_{h,\varepsilon}$, for all $\varphi \in C_c^\infty((t_0, t_2), \mathbb{R}^N \times \mathbb{R}^N)$, the first variation

$$\delta I_{h,\varepsilon}(q, \varphi) = \int_{t_0}^{t_2} \dot{q}^{\mathrm{T}} M \dot{\varphi} - \nabla V_{h,\varepsilon}(q)\varphi \, \mathrm{d}t$$

vanishes. A standard approximation argument shows that this remains true for all $\varphi \in W_0^{1,\infty}((t_0, t_2), \mathbb{R}^N \times \mathbb{R}^N)$. Now suppose that q' is another piecewise linear trajectory with $\tilde{q}(t_0) = q'(t_0)$, $\tilde{q}(t_2) = q'(t_2)$, which is nearby $\tilde{q}$ and meets the same energy jump surface Γ at time t_1'. Choose $\tau_{1,\varepsilon}', \tau_{2,\varepsilon}'$, such that q' enters, resp. leaves, Γ_ε at time $t_1' - \tau_{1,\varepsilon}'$ resp. $t_1' + \tau_{2,\varepsilon}'$

Now construct the following particular approximation q_ε' to q':

- $q_\varepsilon'(t)$ is linear on $(t_0, t_1' - \tau_{1,\varepsilon})$ and on $(t_1' + \tau_{2,\varepsilon}, t_2)$,
- $q_\varepsilon'(t_1' - \tau_{1,\varepsilon}) = q'(t_1' - \tau_{1,\varepsilon}')$ and $q_\varepsilon'(t_1' + \tau_{2,\varepsilon}) - q'(t_1' + \tau_{2,\varepsilon}') \to 0$ as $\varepsilon \to 0$ and
- $V_{h,\varepsilon}(q_\varepsilon'(t_1' + t)) = V_{h,\varepsilon}(q_\varepsilon(t_1 + t))$ for $t \in [-\tau_{1,\varepsilon}, \tau_{2,\varepsilon}]$.

It is not hard to see that, as $\varepsilon \to 0$, $q_\varepsilon' \to q'$ strongly in $W^{1,p}$ for all $p < \infty$ (and weak* in $W^{1,\infty}$), and in particular $I_{h,\varepsilon}(q_\varepsilon) \to I_h(\tilde{q})$, $I_{h,\varepsilon}(q_\varepsilon') \to I_h(q')$. In fact, due to the careful definition of q_ε', we also obtain control over the difference

$$I_{h,\varepsilon}(q_\varepsilon) - I_{h,\varepsilon}(q_\varepsilon') \to I_h(\tilde{q}) - I_h(q')$$

To see this, it suffices to note that

$$\int_{t_1' - \tau_{1,\varepsilon}}^{t_1' + \tau_{2,\varepsilon}} V(q_\varepsilon'(t)) \, \mathrm{d}t - \int_{t_1 - \tau_{1,\varepsilon}}^{t_1 + \tau_{2,\varepsilon}} V(q_\varepsilon(t)) \, \mathrm{d}t = 0$$

In fact, as q_ε is a critical point of $I_{h,\varepsilon}$, we have

$$|I_{h,\varepsilon}(q_\varepsilon) - I_{h,\varepsilon}(q_\varepsilon')| = o(\|q_\varepsilon - q_\varepsilon'\|_{W^{1,2}})$$

with a term $o(\cdot)$ independent of ε. (Consider a path $[0, 1] \ni s \mapsto q_\varepsilon(\cdot, s)$ in the space of curves such that $q_\varepsilon(\cdot, 0) = q_\varepsilon$, $q_\varepsilon(\cdot, 1) = q_\varepsilon'$ and $V_{h,\varepsilon}(q_\varepsilon(t_1(s) + \cdot, s)) = V_{h,\varepsilon}(q_\varepsilon(t_1 + \cdot))$ on $[-\tau_{1,\varepsilon}, \tau_{2,\varepsilon}]$, where $t_1(s)$ interpolates between t_1 and t_1', that is $t_1(0) = t_1$ and $t_1(1) = t_1'$.)

As a consequence we obtain

$$|I_h(\tilde{q}) - I_h(q')| = o(\|\tilde{q} - q'\|_{W^{1,2}})$$

and thus that $\tilde{q}$ is a critical point of the action functional I_h on piecewise linear trajectories as identified in Section 2. Now, as $q(0) = \tilde{q}(0)$ and $\dot{q}(0) = \dot{\tilde{q}}(0)$, we obtain $\tilde{q} = q$. Hence, q is the limit, as $\varepsilon \to 0$ of the smooth trajectories q_ε corresponding to the smooth Lagrangian $L_{h,\varepsilon}$. □

2.3. Summary of the energy-stepping scheme

We close this section by summarizing the relations obtained in the foregoing and defining the *energy-stepping* approximation scheme resulting from a piecewise-constant approximation of the potential energy.

DOI: 10.1002/nme

Definition 2.1 (*Energy-stepping*)
Suppose $(t_k, q_k, \dot{q}_k^+)$ and a piecewise-constant approximation of the potential energy V_h are given. Let t_{k+1} and q_{k+1} be the time and point of exit of the rectilinear trajectory $q_k + (t - t_k)\dot{q}_k^+$ from the set $\{V = h\mathbb{Z}\}$. Let ΔV be the energy jump at q_{k+1} in the direction of advance. The updated velocity is, then,

$$\dot{q}_{k+1}^+ = \dot{q}_k^+ + \lambda_{k+1} M^{-1} n_{k+1} \tag{24}$$

where

$$\lambda_{k+1} = \begin{cases} -2\dfrac{\dot{q}_k^+ \cdot n_{k+1}}{n_{k+1}^T M^{-1} n_{k+1}} \\ \quad \text{if } (\dot{q}_k^+ \cdot n_{k+1})^2 < 2\Delta V (n_{k+1}^{\mathrm{T}} M^{-1} n_{k+1}) \\ \dfrac{-\dot{q}_k^+ \cdot n_{k+1} + \operatorname{sign}(\Delta V)\sqrt{(\dot{q}_k^+ \cdot n_{k+1})^2 - 2\Delta V (n_{k+1}^{\mathrm{T}} M^{-1} n_{k+1})}}{n_{k+1}^{\mathrm{T}} M^{-1} n_{k+1}} \\ \quad \text{otherwise} \end{cases} \tag{25}$$

Algorithm 1 Energy-stepping scheme

Require: $V(q)$, q_0, $\dot{q}_0$, t_0, t_f and the energy step h
1. $i \leftarrow 0$
2. **while** $t_i < t_f$ **do**
3. $\quad t_{i+1} \leftarrow$ SMALLEST-ROOT$(V(q_i + (t_{i+1} - t_i)\dot{q}_i) - V(q_i) + \Delta V = 0)$
4. $\quad q_{i+1} \leftarrow q_i + (t_{i+1} - t_i)\dot{q}_i$
5. $\quad n_{i+1} \leftarrow \nabla V(q_{i+1})$
6. $\quad \dot{q}_{i+1} \leftarrow$ UPDATE-VELOCITIES$(\dot{q}_i, n_{i+1}, h)$
7. $\quad i \leftarrow i + 1$
8. **end while**

These relations define a discrete propagator

$$\Phi_h : (t_k, q_k, \dot{q}_k^+) \mapsto (t_{k+1}, q_{k+1}, \dot{q}_{k+1}^+) \tag{26}$$

that can be iterated to generate a discrete trajectory.

The implementation of the energy-stepping scheme is summarized in Algorithm 1. The algorithm consists of two methods. The first method SMALLEST-ROOT determines the earliest root of the equation

$$V(q_i + (t_{i+1} - t_i)\dot{q}_i) - V(q_i) + \Delta V = 0 \tag{27}$$

where ΔV can take values in $\{0, h, -h\}$. This task can be effectively accomplished by locating first, by means of an incremental search technique, a time interval containing the smallest positive root and then zeroing in on the root by means of an iterative procedure such as bisection, Newton–Raphson or a combination thereof. The nature of the step, that is whether it consists of a diffraction by an uphill energy step, a diffraction by a downhill energy step or a reflection at an uphill energy

DOI: 10.1002/nme

step, is identified simultaneously with the computation of t_{i+1}. The second method UPDATE-VELOCITIES is responsible for updating velocities according to Definition 2.1 and reduces to only two scenarios. The method is defined in Algorithm 2.

Algorithm 2 UPDATE-VELOCITIES$(\dot{q}_0, n_1, h)$

1. **if** $\dot{q}_0 \cdot n_1 \geqslant 0$ **then**
2. $\quad \Delta V \leftarrow h$ // Positive energy jump approached
3. **else**
4. $\quad \Delta V \leftarrow -h$ // Negative energy jump approached
5. **end if**
6. **if** $(\dot{q}_0 \cdot n_1)^2 \leqslant 2\Delta V (n_1^T M^{-1} n_1)$ **then**
7. $\quad \lambda \leftarrow -2\frac{\dot{q}_0 \cdot n_1}{n_1^T M^{-1} n_1}$ // Reflects back from energy barrier
8. **else**
9. $\quad \lambda \leftarrow \frac{-\dot{q}_0 \cdot n_1 + \text{sign}(\Delta V)\sqrt{(\dot{q}_0 \cdot n_1)^2 - 2\Delta V (n_1^T M^{-1} n_1)}}{n_1^T M^{-1} n_1}$ // Overcomes energy jump
10. **end if**
11. **return** $\dot{q}_0 + \lambda M^{-1} n_1$

It bears emphasis that energy-stepping requires the solution of no system of equations and, therefore, its complexity is comparable to that of explicit methods. However, the need to compute the root of a nonlinear function adds to the overhead of one application of the algorithm. It is still possible, however, that such overhead may be offset by the higher accuracy in particular applications. These and other trade-offs are investigated subsequently by way of numerical testing.

3. CONSERVATION PROPERTIES

Because the stepwise approximation of the potential energy (4) preserves all the symmetries of the system, and the discrete trajectories are exact trajectories of a Lagrangian system, energy-stepping exactly conserves all the momentum maps and the symplectic structure of the original Lagrangian system. These two types of conservation properties are examined next in turn.

3.1. Conservation of momentum maps

The theory of symmetry of smooth Lagrangian systems is well-known [17] but may stand a brief summary, specifically as it bears on the present application. We recall that a Lagrangian is a function $L : TQ \to \mathbb{R}$, where Q is a smooth, or configuration, manifold of the system and TQ is the corresponding tangent bundle, consisting of pairs of configurations and velocities. For simplicity, we restrict attention to time-independent or autonomous Lagrangians. Let X denote some suitable topological space of trajectories $q : [0, T] \to Q$ joining fixed initial and final configurations $q(0)$ and $q(T)$, respectively. Then, the action integral $I : X \to \mathbb{R}$ over the time interval $[0, T]$ is

$$I(q) = \int_0^T L(q(t), \dot{q}(t))\, \mathrm{d}t \tag{28}$$

DOI: 10.1002/nme

where we assume sufficient regularity of L and $q(t)$ for all mathematical operations to be well defined. According to Hamilton's principle, the physical trajectories of the system are the critical points of I, that is $q \in X$ is a trajectory if

$$\delta I(q, \varphi) = 0 \tag{29}$$

for all variations $\varphi \in C_c^\infty(0, T)$. Throughout this paper the configurational space of interest is $Q = E(n)^N$, where $E(n)$ is the Euclidean space of dimension n, and the Lagrangian is assumed to be of the form (1), with V smooth and bounded below, or (2) with V_h piecewise constant. An appropriate space of trajectories is $X = W^{1,p}([0, T])$, $p < \infty$, as demonstrated in Section 4. We note that in the case of a piecewise-constant potential energy the Lagrangian is not differentiable and the Euler–Lagrange equations are not defined in the classical sense. However, the trajectories can still be understood as critical points of the action functional I_h as shown in Theorem 2.1.

Let G be a Lie group with Lie algebra $\mathfrak{g} = T_e G$. A left action of G on Q is a mapping $\Phi : G \times Q \to Q$ such that: (i) $\Phi(e, \cdot) = \mathrm{id}$; ii) $\Phi(g, \Phi(h, \cdot)) = \Phi(gh, \cdot)$ $\forall g, h \in G$. Let $\xi \in \mathfrak{g}$. Then, the infinitesimal generator of Φ corresponding to ξ is the vector field $\xi_Q \in TQ$ given by

$$\xi_Q(q) = \frac{\mathrm{d}}{\mathrm{d}t}[\Phi(\exp(t\xi), q)]_{t=0} \tag{30}$$

The momentum map $J : TQ \to \mathfrak{g}^*$ defined by the action Φ then follows from the identity

$$\langle J(q, \dot{q}), \xi \rangle = \langle \partial_{\dot{q}} L(q, \dot{q}), \xi_Q(q) \rangle \quad \forall \xi \in \mathfrak{g} \tag{31}$$

We say that the Lagrangian L is invariant under the action Φ if

$$L(\Phi_g(q), T\Phi_g(q)\dot{q}) = L(q, \dot{q}) \quad \forall g \in G, \quad (q, \dot{q}) \in TQ \tag{32}$$

where we write $\Phi_g(\cdot) = \Phi(g, \cdot)$. Under these conditions, we additionally say that G is a symmetry group of the system and that Φ expresses a symmetry of the system. The classical theorem of Noether states that if L is invariant under the action Φ, then the corresponding momentum map J is a constant of the motion, that is it remains constant along the trajectories. Classical examples include:

(i) *Conservation of linear momentum*. In this case, $Q = E(n)^N$, $G = E(n)$ and $\Phi(u, q) = \{q_1 + u, \ldots, q_N + u\}$ represent a rigid translation of the system by $u \in E(n)$. The corresponding momentum map is the total linear momentum of the system, $J = p_1 + \cdots + p_N$. If the Lagrangian is invariant under translations, then the total linear momentum is a constant of the motion.

(ii) *Conservation of angular momentum*. In this case, $Q = E(n)^N$, $G = SO(n)$ and $\Phi(R, q) = \{Rq_1, \ldots, Rq_N\}$ represent a rigid rotation of the system by $R \in SO(n)$. The corresponding momentum map is the total angular momentum of the system, $J = q_1 \times p_1 + \cdots + q_N \times p_N$. If the Lagrangian is invariant under rotations, then the total angular momentum is a constant of the motion.

Conservation of energy can be fit into this framework by resorting to a space–time formulation in which time is regarded as a generalized coordinate, for example q_0. The corresponding space–time Lagrangian is $\mathbb{L}(\mathbb{q}, \mathbb{q}') = \mathbb{L}((q_0, q), (q_0', q')) = L(q, q'/q_0', q_0)$, where $L(q, \dot{q}, t)$ is a general time-dependent Lagrangian. The space–time configuration manifold is $\mathbb{Q} = \mathbb{R} \times Q$. Let $G = \mathbb{R}$, $\Phi(s, q) = (q_0 + s, q)$ is a time-shift and suppose that $\mathbb{L}$ is invariant under Φ, that is L is

DOI: 10.1002/nme

time-independent. Then $J = L - \partial_{\dot{q}} L \cdot \dot{q} = -E$, that is the total energy of the system, is a constant of the motion.

A particularly appealing property of the piecewise-constant approximation (4) of the potential energy is that it preserves all the symmetries of the system exactly. To verify this property, as the kinetic energy of the system is not approximated, it suffices to verify that V_h has all the symmetries of V. Thus, suppose that G is a symmetry group of V and Φ is an action that leaves V invariant, that is,

$$V \circ \Phi_g = V \quad \forall g \in G \tag{33}$$

Then,

$$V_h \circ \Phi_g = (h \lfloor h^{-1} V \rfloor) \circ \Phi_g = h \lfloor h^{-1} V \circ \Phi_g \rfloor = h \lfloor h^{-1} V \rfloor = V_h \tag{34}$$

Similarly, we obtain for the smooth approximation of V_h introduced in (22)

$$V_{h,\varepsilon} \circ \Phi_g = \chi_\varepsilon \circ V \circ \Phi_g = \chi_\varepsilon \circ V = V_{h,\varepsilon} \tag{35}$$

It therefore follows from Noether's theorem that the corresponding momentum map J is constant along trajectories of the approximate Lagrangian $L_{h,\varepsilon}$. By Theorem 2.1 and a standard approximation argument then show that the momentum map J is constant along energy-stepping trajectories. It bears emphasis that what is conserved along the trajectories of the approximate Lagrangian L_h is the *exact*, time-continuous, momentum map of the original Lagrangian L. This is in contrast to discrete variational integrators, which conserve a discrete form of the momentum maps, instead of the exact, time-continuous, momentum maps of the original Lagrangian L. Thus, in particular: if V is invariant under translations then energy-stepping conserves the total linear momentum $p_1 + \cdots + p_N$ of the system; and if V is invariant under rotations then energy-stepping conserves the total angular momentum $q_1 \times p_1 + \cdots + q_1 \times p_N$ of the system.

As indicated above, the exact conservation of energy attendant to energy-stepping applied to time-independent Lagrangians follows in the manner described above from a space–time extension of the configuration manifold. However, exact energy conservation follows more directly as a consequence of (12), that is energy conservation is built explicitly into the energy-stepping scheme.

3.2. Conservation of the symplectic structure

We now look at the Lagrangian systems defined by (1) and (2) from a Hamiltonian perspective. To this end we introduce the phase space $P = T^*Q$, consisting of pairs (q, p) of configurations $q \in Q = E(n)^N$ and momenta $p \in T_q^* Q$, and the Hamiltonian $H : P \to \mathbb{R}$ as

$$H(q, p) = \sup_{v \in T_q Q} \{p \cdot v - L(q, v)\} = \frac{1}{2} p^{\mathrm{T}} M^{-1} p + V(q) \tag{36}$$

Likewise, the Hamiltonian corresponding to the approximate Lagrangian (2) is

$$H_h(q, p) = \sup_{v \in T_q Q} \{p \cdot v - L_h(q, v)\} = \frac{1}{2} p^{\mathrm{T}} M^{-1} p + V_h(q) \tag{37}$$

We endow P with the canonical *symplectic two-form*

$$\Omega = dq_1 \wedge dp_1 + \cdots + dq_N \wedge dp_N \tag{38}$$

Then, the pair (P, Ω) defines a symplectic manifold.

DOI: 10.1002/nme

We recall (cf. e.g. [18–20]) that a diffeomorphism $\varphi: P \to P$ is *symplectic* if it preserves the symplectic two-form, that is, if

$$\Omega(T\varphi(z)\eta_1, T\varphi(z)\eta_2) = \Omega(\eta_1, \eta_2) \tag{39}$$

The symplecticity of Lipschitz maps has been investigated by Whitney [21] and by Gol'dshtein and Dubrovskiy [22], but their results do not apply to the present setting. However, it is possible to verify the symplecticity of energy-stepping directly. To this end, we may write $\varphi(q_0, p_0) = (q(t), p(t))$ and

$$T\varphi \equiv \begin{pmatrix} \partial_q \varphi_q & \partial_p \varphi_q \\ \partial_q \varphi_p & \partial_p \varphi_p \end{pmatrix} = \begin{pmatrix} Q_q & Q_p \\ P_q & P_p \end{pmatrix} \tag{40}$$

then φ is symplectic if

$$P_p^{\mathrm{T}} Q_p = Q_p^{\mathrm{T}} P_p \tag{41}$$

$$P_p^{\mathrm{T}} Q_q = Q_p^{\mathrm{T}} P_q + I \tag{42}$$

$$Q_q^{\mathrm{T}} P_q = P_q^{\mathrm{T}} Q_q \tag{43}$$

As shown in the appendix, these relations are identically satisfied by energy-stepping, which establishes the symplecticity of the scheme.

3.3. Summary of the conservation properties of the energy-stepping scheme

The results proven in the foregoing are collected and summarized in the following theorem.

Theorem 3.1
The energy-stepping time-integration scheme is a symplectic-energy-momentum time-reversible integrator with automatic selection of the time-step size. In particular, the scheme conserves exactly all the momentum maps of the original Lagrangian.

Symmetry or time-reversibility of energy-stepping follows directly from the definition of the scheme. The automatic time-step selection property also follows by construction. In particular, in regions where the potential energy gradient ∇V is steep, the energy jumps are more closely spaced and the resulting time steps are small. By contrast, if the potential energy gradient is small, the resulting time steps are comparatively large. We again emphasize that the momentum maps conserved by energy-stepping are precisely those conserved by the original system. This is in contrast to variational integrators, which conserve discrete momentum maps that differ from the momentum maps of the original system in general.

4. CONVERGENCE ANALYSIS

Our aim in this section is to ascertain conditions under which a sequence q_h of energy-stepping trajectories with potential V_h and initial conditions $q_h(0) = q_0$ and $\dot{q}_h(0+) = \dot{q}_0$ converges in a suitable sense to a solution q of the original equations of motion as $h \to 0$. For the sake of simplicity, we consider the motion $t \mapsto q(t) \in \mathbb{R}^N$ of a particle in a smooth potential energy landscape V with

DOI: 10.1002/nme

diagonal mass matrix of the form $M = m\mathrm{Id}$. The convergence analysis presented in the following carries over unchanged to the general case, albeit at the expense of slightly more cumbersome notation. The trajectories q are stationary points of the action functional

$$I(q) = \int_0^T \frac{m}{2}(\dot{q}(t))^2 - V(q(t))\,\mathrm{d}t \tag{44}$$

For smooth trajectories, this principle is equivalent to the satisfaction of the equations of motion

$$m\ddot{q}(t) = -\nabla V(q(t)), \quad q(0) = q_0, \quad \dot{q}(0) = \dot{q}_0 \quad \text{given} \tag{45}$$

We will assume throughout that V is bounded from below and, without loss of generality, we may specifically assume that $V \geqslant 0$.

Within this setting, the aim of convergence analysis is to elucidate the limiting behavior of the stationary points of the approximating functionals I_h that arise when the smooth potential V is approximated by piecewise-constant potentials V_h. However, due to the non differentiability of V_h, the first variation

$$\delta I_h(q, \varphi) := \lim_{s \to 0} \frac{1}{s}\left(\int_0^T \frac{m}{2}(\dot{q} + s\dot{\varphi})^2 - V_h(q + s\varphi)\,\mathrm{d}t - \int_0^T \frac{m}{2}(\dot{q})^2 - V_h(q)\,\mathrm{d}t \right) \tag{46}$$

does not exist in general for arbitrary $\varphi \in C_c^\infty(0, t; \mathbb{R}^N)$. The equation of motion (45) needs to be adapted to this situation by allowing the approximating acceleration to be a measure, specifically, a sum of suitably rescaled Dirac masses. With this extension, we may summarize the energy-stepping scheme formulated in Section 2.3 by saying that the approximating sequences satisfy the Euler-Lagrange equations

$$m\ddot{q} = \sum_{t \in S(q)} \alpha(q(t), \dot{q}(t-), \dot{q}(t+)) n(q(t)) \delta_t \tag{47}$$

in the sense of $\mathbb{R}^N$-valued measures, where

$$\alpha(q(t), \dot{q}(t-), \dot{q}(t+)) = \begin{cases} -2m\dot{q}(t-) \cdot n(q(t)) & \text{if } \sqrt{\dfrac{2h}{m}} > \dot{q}(t-) \cdot n(q(t)) > 0 \\ \dfrac{-h}{\left| \dfrac{\dot{q}(t+) + \dot{q}(t-)}{2} \cdot n(q(t)) \right|} & \text{otherwise} \end{cases} \tag{48}$$

$n(q) = \nabla V(q)/|\nabla V(q)|$ and $S(q)$ denotes the set of times t where $\dot{q}(t)$ jumps. Indeed, as $\dot{q}$ is only piecewise constant, $\ddot{q}$ is only defined as a distribution. In order to identify $\ddot{q}$, let $\varphi : (0, \infty) \to \mathbb{R}^N$ be a smooth, compactly supported function. We have to verify that

$$\begin{aligned} -\int_0^\infty m\dot{q}(s) \cdot \dot{\varphi}(s)\,\mathrm{d}s &= \int_0^\infty \varphi(s) \cdot \mathrm{d}\left(\sum_{t \in S(q)} \alpha(q(t), \dot{q}(t-), \dot{q}(t+)) n(q(t)) \delta_t \right)(s) \\ &= \sum_{t \in S(q)} \alpha(q(t), \dot{q}(t-), \dot{q}(t+)) n(q(t)) \cdot \varphi(t) \end{aligned} \tag{49}$$

In fact, by recourse to a partition of unity it suffices to verify this identity for φ supported on intervals (t', t'') that contain at most one point of $S(q)$. If $S(q) \cap (t', t'') = \emptyset$, then $\dot{q}$ is constant on

DOI: 10.1002/nme

(t', t'') and both sides of (49) are zero. Now let $S(q) \cap (t', t'') = \{t\}$ and denote the velocity $\dot{q}$ prior to t, resp. after t, by $\dot{q}(t-)$, resp. $\dot{q}(t+)$. Then (49) is equivalent to

$$-\int_{t'}^{t''} m\dot{q}(s) \cdot \dot{\varphi}(s)\, \mathrm{d}s = \alpha(q(t), \dot{q}(t-), \dot{q}(t+)) n(q(t)) \cdot \varphi(t) \tag{50}$$

Splitting the integral as $\int_{t'}^{t} + \int_{t}^{t''}$ we obtain

$$-\int_{t'}^{t''} m\dot{q}(s) \cdot \dot{\varphi}(s)\, \mathrm{d}s = m(\dot{q}(t+) - \dot{q}(t-)) \cdot \varphi(t) \tag{51}$$

and Equation (49) follows with

$$\alpha n = m(\dot{q}(t+) - \dot{q}(t-)) \tag{52}$$

This identity in turn is consistent with the more direct approach followed in Section 2.3. Indeed, if the trajectory reflects at an energy level surface, (52) is directly implied by Definition 2.1. If, contrariwise, an energy level surface is crossed Definition 2.1 gives

$$m(\dot{q}(t+) - \dot{q}(t-)) = m(-\dot{q}(t-) \cdot n + \mathrm{sign}(\Delta V)\sqrt{(\dot{q}(t-) \cdot n)^2 - 2\Delta V m^{-1}})n =: \lambda n \tag{53}$$

with $\Delta V = V_h(q(t+)) - V_h(q(t-))$, $h = |\Delta V|$. Multiplying with $\dot{q}(t-) + \dot{q}(t+)$, we obtain from Equation (12)

$$-2\Delta V = m((\dot{q}(t+))^2 - (\dot{q}(t-))^2) = \lambda(\dot{q}(t-) + \dot{q}(t+)) \cdot n \tag{54}$$

whence indeed

$$\lambda = \frac{-\Delta V}{\dfrac{\dot{q}(t+) + \dot{q}(t-)}{2} \cdot n} = \frac{-h}{\left|\dfrac{\dot{q}(t+) + \dot{q}(t-)}{2} \cdot n\right|} = \alpha \tag{55}$$

In general, the approximating sequences thus defined may fail to converge to trajectories of the original system as $h \to 0$. The nature of the difficulty is illustrated by the following three examples.

4.1. Failure of convergence

The first example shows that the convergence does not necessarily hold true even for one-dimensional problems.

Example 4.1

For definiteness suppose that $m = 1$, $q_0 = 0, \dot{q}_0 = 1$ and V is given by $V(x) = \frac{1}{2}x^2$. Then (45) describes an harmonic oscillator and the trajectory is $q(t) = \sin(t)$. Similarly, q_h increases monotonically as long as $V^h(q_h) < \frac{1}{2}$. Let $k = \lfloor 1/2h \rfloor$. Then on $\{t : q_h(t) \in (\sqrt{2kh}, \sqrt{2(k+1)h})\}$ the approximating velocity is

$$\dot{q}_h = \sqrt{1 - 2kh} \tag{56}$$

DOI: 10.1002/nme

and the time from reaching the top energy level kh until bouncing at $q_h = \sqrt{2(k+1)h}$ is

$$\Delta t = \frac{\sqrt{2(k+1)h} - \sqrt{2kh}}{\sqrt{1-2kh}} \approx \frac{h}{\sqrt{\frac{1}{2} - kh}} \tag{57}$$

In particular, q_h does not converge to q if the last expression does not converge to zero as $h \to 0$.

This example shows that there may be sequences h_i such that the stationary trajectories of I_{h_i} do not converge to stationary trajectories of I. Of course, this does not rule out the existence of sequences h_i for which convergence does take place, and non convergence situations of the type illustrated by the example can be readily avoided by a proper choice of sequence. The second example shows that convergence of q_h to q may fail due to *non transversality* of the velocity with respect to ∇V.

Example 4.2
Let $V : \mathbb{R}^2 \to \mathbb{R}_+$ and suppose that $V(x, y) = \frac{1}{2}x^2$. If $m = 1$, $q_0 = (1, 0)^{\mathrm{T}}, \dot{q}_0 = (0, 1)^{\mathrm{T}}$, then the solution q of (45) is given by $q(t) = (\cos(t), t)^{\mathrm{T}}$. However, the solutions q_h of (47) are uniform motions in the y-direction, that is $q_h(t) = (0, t)^T$, independently of h.

While in this example the lack of convergence is due to the approximating trajectories not *feeling* the force in the x-direction, we show in the last example that even if there are no long time intervals over which none of the level sets $\{V = kh\}$ is hit, the approximating trajectory may fail to converge to a solution of (45).

Example 4.3
Let $V : \mathbb{R}^2 \to \mathbb{R}_+$, $V(x, y) = \frac{1}{2}(x^2 + y^2)$ and assume that $m = 1$, $q_0 = (1, 0)^{\mathrm{T}}$ and $\dot{q}_0 = (0, \gamma)^{\mathrm{T}}$, $\gamma > 0$. Let $k = \lfloor 1/2h \rfloor$. Elementary geometric considerations show that $\mathrm{dist}(q_0, \{V = (k+1)h\}) \leqslant h + o(h)$ and, if q_h hits the set $\{V = (k+1)h\}$, then $\gamma\sqrt{2h} + o(\sqrt{h}) > \dot{q}_h(t-) \cdot n(q(t)) > 0$. If $\gamma < 1$, then q_h bounces and then indeed q_h bounces whenever it hits the set $\{V = (k+1)h\}$, that is the trajectory describes a polygon approximating the circle with radius 1 centered at 0. However, the solution q of the continuum problem is $q(t) = (\cos(t), \gamma \sin(t))^{\mathrm{T}}$ and, hence, for $\gamma < 1$, q_h cannot converge to q (see Figure 3 for an illustration).

These examples suggest that the lack of convergence is connected to a very slow motion in the direction parallel to ∇V. As observed in Section 4.3, in one dimension this can be overcome by a suitable selection of the initial conditions. This is due to the fact that in one dimension, energy conservation furnishes a one-to-one correspondence between the initial velocity and the velocity at a later time near a turning point. Analogously in higher dimensions, a proper choice of the initial conditions could remedy the lack of the convergence that might appear at the first point the continuum trajectory becomes non transversal to an energy jump surface. However, there seems to be no natural condition that would guarantee convergence also at later turning points. (Note that energy conservation only gives control over the absolute value $|\dot{q}|$. In higher dimension $|\dot{q} \cdot \nabla V|$ can be very small even if $|\dot{q}|$ is large.) Examples 4.2 and 4.3 have to be understood in this vein: Even if the trajectory is well behaved initially on the time interval $[0, t_0]$, say, convergence might fail after time $t_0 > 0$. This is indeed the case if $(q(t_0), \dot{q}(t_0))$ assumes the value denoted $(q_0, \dot{q}_0)$ in Example 4.2 or 4.3.

DOI: 10.1002/nme

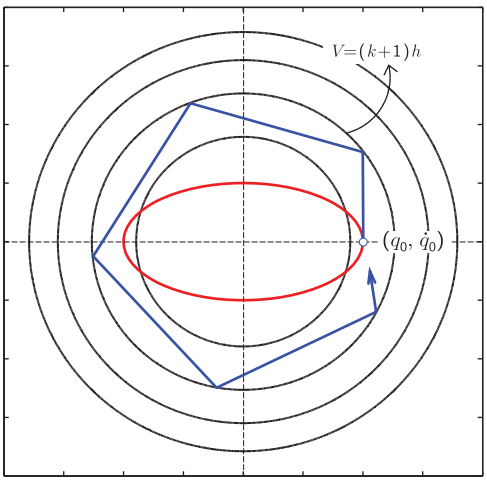

Figure 3. Illustration of Example 3.3. Red line: Exact solution. Blue line: Energy-stepping solution.

4.2. *Convergence of transversal trajectories*

In view of the preceding examples we introduce the following definition.

Definition 4.1
Let q_h be a sequence of solutions of (47) and set $\Delta q_{hi} := q_h(t_{i+1}) - q_h(t_i)$, where $S(q_h) = \{t_1, \ldots, t_{N_h}\}$ is the jump set of $\dot{q}_h(t)$. We say that q_h is transversal if

$$\lim_{h\to 0} \min_i \frac{|n(t_i)\cdot \dot{q}_h(t_i-)|}{\sqrt{h}} = \infty \quad \text{and} \quad \lim_{h\to 0} \max_i \frac{|\Delta q_{hi}|}{\sqrt{h}} = 0$$

Then, we have the following convergence result.

Theorem 4.4
Let q_0 and $\dot{q}_0$ be given such that $\nabla V(q_0)\cdot \dot{q}_0 \neq 0$ and suppose q_h solves (47) with $q_h(0) = q_0$ and $\dot{q}_h(0+) = \dot{q}_0$ for $h>0$. Then if the sequence q_h is transversal, $q_h \to q$ in $W^{1,p}(0,T)$ for each fixed $T>0$ and all $p<\infty$, where q is the unique solution of (45).

Proof
Since V is bounded from below, we have

$$\|q_h\|_{L^\infty}, \|\dot{q}_h\|_{L^\infty} \leqslant C$$

for some constant C independent of h. Therefore, by passing if necessary to a subsequence we can assume that

$$q_h \overset{*}{\rightharpoonup} q \quad \text{in } W^{1,\infty}$$

DOI: 10.1002/nme

for some $q \in W^{1,\infty}$, and thus $q_h \to q$ uniformly. Let $\varphi \in C([0,T];\mathbb{R}^N)$. Then

$$\int_0^T h \sum_{t\in S(q_h)} \alpha(q_h(\tau), \dot{q}_h(\tau-), \dot{q}_h(\tau+)) n(q_h(\tau)) \cdot \varphi(\tau) \delta_t(d\tau)$$

$$= h \sum_{i=1}^{N_h} \alpha(q_h(t_i), \dot{q}_h(t_i-), \dot{q}_h(t_i+)) n(q_h(t_i)) \cdot \varphi(t_i)$$

where $t_1 < t_2 < \cdots < t_N$ are such that $\{t_1, \ldots, t_N\} = S(q_h) = \{t : V(q_h(t)) \in h\mathbb{N}\}$. By transversality, $|\Delta q_{hi}| \to 0$ as $h \to 0$ uniformly in i and $\dot{q}_h(t_i+) \cdot n(q_h(t_{i+1})) = \dot{q}_h(t_{i+1}-) \cdot n(q_h(t_{i+1})) \notin (0, \sqrt{2h/m})$. Therefore, we have

$$\begin{aligned} h &= |V(q_h(t_{i+1})) - V(q_h(t_i))| \\ &= |\nabla V(q_h(t_i)) \cdot \Delta q_{hi} + \tfrac{1}{2} D^2 V(\lambda_i q_h(t_i) + (1-\lambda_i)(t_{i+1}))(\Delta q_{hi})^2| \\ &= |\nabla V(q_h(t_i)) \cdot \dot{q}_h(t_i+)(t_{i+1} - t_i) + \tfrac{1}{2} D^2 V(q_h(\tau_i))(\Delta q_{hi})^2| \end{aligned}$$

for some $\lambda_i \in (0,1)$, resp., $\tau_i \in (t_i, t_{i+1})$. Again, by transversality we obtain

$$h = |\nabla V(q_h(t_i)) \cdot \dot{q}_h(t_i+)|(t_{i+1} - t_i) + o(h)$$

Next we note that $|\alpha| \leqslant C\sqrt{h}$ since, if $\dot{q}(t-) \cdot n(q(t)) \geqslant \sqrt{2h/m}$, then

$$\frac{\dot{q}(t+) + \dot{q}(t-)}{2} \cdot n(q(t)) \leqslant \frac{\dot{q}(t-)}{2} \cdot n(q(t)) \tag{58}$$

whereas, if $\dot{q}(t-) \cdot n(q(t)) \leqslant 0$, then

$$\frac{\dot{q}(t+) + \dot{q}(t-)}{2} \cdot n(q(t)) \leqslant \frac{\dot{q}(t+)}{2} \cdot n(q(t)) \leqslant -C\sqrt{h} \tag{59}$$

From these bounds we obtain $|\dot{q}_h(t_i-) - \dot{q}_h(t_i+)| \leqslant C\sqrt{h}$. As $|n(t_i) \cdot \dot{q}_h(t_i-)| \gg \sqrt{h}$, this in turn implies that

$$h = \left| \nabla V(q_h(t_i)) \cdot \frac{\dot{q}_h(t_i-) + \dot{q}_h(t_i+)}{2} \right| (t_{i+1} - t_i) + o(h)$$

It now follows that

$$\int_0^T h \sum_{t\in S(q_h)} \frac{\nabla V(q_h(\tau)) \cdot \varphi(\tau)}{\left| \nabla V(q_h(\tau)) \cdot \dfrac{\dot{q}_h(\tau+) + \dot{q}_h(\tau-)}{2} \right|} \delta_t(\mathrm{d}\tau)$$

$$= h \sum_{i=1}^{N_h} \frac{\nabla V(q_h(t_i)) \cdot \varphi(t_i)}{\left| \nabla V(q_h(t_i)) \cdot \dfrac{\dot{q}_h(t_i+) + \dot{q}_h(t_i-)}{2} \right|}$$

$$= \sum_{i=1}^{N_h} \nabla V(q_h(t_i)) \cdot \varphi(t_i)(t_{i+1} - t_i) + o(1)$$

DOI: 10.1002/nme

where we note that $N_h \leqslant Ch^{-1}$. As $q_h \to q$ uniformly as $h \to 0$ and

$$\max_i |t_{i+1} - t_i| \leqslant \frac{|\Delta q_{hi}|}{|\dot{q}_h(t_{i+1}-)|} \ll \frac{\sqrt{h}}{\sqrt{h}} = 1 \tag{60}$$

we obtain by a Riemann sum argument that the last term converges to

$$\int_0^T \nabla V(q(t)) \cdot \varphi(t)\, \mathrm{d}t \tag{61}$$

We have thus shown that the right-hand side of (47) converges weak-* in measure to $-\nabla V(q)$. But then, as $\ddot{q}_h \to \ddot{q}$ in the sense of distributions, we can take the limit $h \to 0$ on both sides of the Euler–Lagrange Equations (47) to conclude that q satisfies the limiting equation

$$m\ddot{q}(t) = -\nabla V(q(t))$$

We next have to show that q satisfies the proper initial conditions. Clearly $q(0) = q_0$ since $q_h \to q$ uniformly. To prove $\dot{q}(0) = \dot{q}_0$, we may assume, without loss of generality, that $\dot{q}_0 \cdot n(x) \geqslant c$ for some $c > 0$ and all x in a neighborhood $\mathscr{U}$ of q_0 (the case $\leqslant -c$ is analogous). As the velocities are bounded in terms of V and $\dot{q}_0$, we may choose $s > 0$ such that $q_h(t) \in \mathscr{U}$ for all $h > 0$ and all $t \in [0, s]$. Now let $s_h \in S(q_h)$ be the smallest time in $[0, s]$ such that $\dot{q}_h(s_h+) \cdot n(q(s_h)) \leqslant c/2$ if such a time exists, $s_h := s$ otherwise. Then, since $\#(S(q_h) \cap [0, s_h]) \leqslant C s_h h^{-1}$ and $\alpha \leqslant Ch$ on $q_h|_{(0,s)}$, it follows that

$$|\dot{q}_h(t) - \dot{q}_h(\tilde{t})| \leqslant C s_h \quad \text{for } t, \tilde{t} \in [0, s_h] \tag{62}$$

In particular, if $s_h < s$, then $|\dot{q}_0 - \dot{q}_h(s_h+)| \geqslant c/2$ and therefore $s_h \geqslant C$ for some constant $C > 0$. Choosing s sufficiently small, again from (62) we deduce that

$$|\dot{q}_h(0+) - \dot{q}_h(t)| \leqslant Cs \quad \text{for } t \in [0, s]$$

and, since $\dot{q}_h|_{[0,s]} \rightharpoonup \dot{q}|_{[0,s]}$ in $L^\infty(0, T)$,

$$|\dot{q}_h(0+) - \dot{q}(t)| \leqslant Cs \quad \text{for } t \in [0, s]$$

Now sending $s \to 0$ proves the claim. By the uniqueness of the solutions of (45), we additionally conclude that the entire sequence q_h converges weak-* to q in $W^{1,\infty}$. But then $q_h \to q$ uniformly and, hence, $\|\dot{q}_h\|_{L^2}^2 \to \|\dot{q}\|_{L^2}^2$ since

$$\tfrac{1}{2}(\dot{q}_h)^2 + V(q_h) = E_h \to E = \tfrac{1}{2}(\dot{q})^2 + V(q)$$

By virtue of the boundedness of $|\dot{q}_h|$, the convergence is indeed strong in $W^{1,p}$ for all $p < \infty$. □

4.3. Discussion of the transversality condition

We conclude this section with a formal argument that, for generic initial data, we may expect convergence of the approximating trajectories beyond turning points. This conjecture is born out by the numerical tests presented in subsequent sections, which suggest that the energy-stepping trajectories may be expected to converge in practice.

In one dimension the argument can be made precise. Assume that $\dot{q}_h(0) \neq 0$. Then, the conserved total energy of the system is $E = (m/2)\dot{q}_0^2 + V_h(q_0)$ and the exact trajectory is a periodic motion

DOI: 10.1002/nme

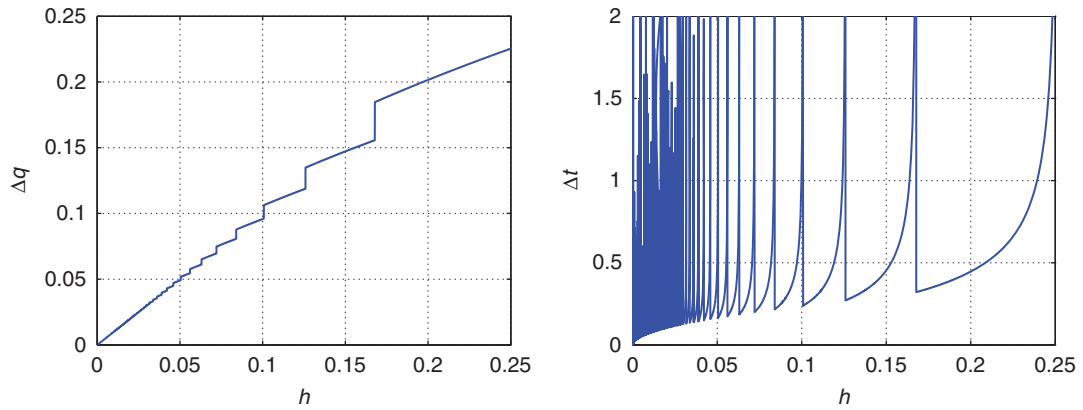

Figure 4. The behavior of $\Delta t(h)$ near a turning point.

between two turning points. We additionally suppose that $V' \neq 0$ at the turning points. Within a finite time interval these points are met finitely often. Under these conditions, convergence fails if and only if the time spent by the trajectory on the highest energy level near the turning points does not converge to zero. As in Example 4.1, we see that such is the case if and only if

$$\limsup_{h\to 0} \Delta t = \limsup_{h\to 0} \frac{\Delta q}{\sqrt{2\dfrac{E-kh}{m}}} \neq 0 \tag{63}$$

with $k = \lfloor E/h \rfloor$ and $\Delta q = q_{k+1} - q_k$ with $V(q_k) = kh$ and $V(q_{k+1}) = kh + h$. Now for Δq near a turning point q we obtain

$$\Delta q = \frac{h}{V'(q)} + O(h^2) \tag{64}$$

and Δq scales with h. From (63), it follows that convergence fails if

$$\liminf_{h\to 0} \frac{E-kh}{h^2} < \infty \tag{65}$$

However, generically $E - kh$ is of the order h. The probability of spending a finite amount of time near a turning point is therefore asymptotically less than $h^\alpha \ll 1$ for any $\alpha < 1$. Thus, as surmised in connection with Example 4.1, it is always possible to select sequences h_i such that the stationary trajectories of I_{h_i} converge to trajectories of I. Figure 4 illustrates the typical behavior of $\Delta t(h)$ when the trajectory is in the vicinity of a turning point. It is evident in the figure that $\Delta t(h)$ indeed becomes vanishingly small as $h \to 0$ on the complement of an exceptional set of small measure.

In arbitrary dimension, for smooth V the motion near a turning point q may be decomposed into a component parallel to the energy jump surface and a transverse component in the direction of $\nabla V(q)$ (cf. Equation (23)). In this transverse direction, the motion is ostensibly one-dimensional and we expect that the preceding argument applies. In order to render this formal argument rigorous we would need an estimate ensuring that the energy associated with the transverse motion at the turning point is not too small. However, no such estimate is known to us for general systems.

DOI: 10.1002/nme

5. NUMERICAL EXAMPLES

Next, we present selected examples of application that showcase the conservation, accuracy, long-term behavior and convergence properties of energy-stepping. We select two areas of application where those properties play an important role. For instance, a good long-term behavior is essential for the purposes of computing equilibrium thermodynamic properties in molecular dynamics. Good energy conservation properties are likewise important in elastic collision problems, especially in many-body problems where the fine structure of collisions may influence significantly the overall behavior of the system. We illustrate the performance of energy-stepping in those areas of application by means of three examples: the dynamics of a frozen argon cluster, the dynamics of a spinning elastic cube, and the dynamics of two colliding elastic spheres.

5.1. Frozen argon cluster

Molecular dynamics falls squarely within the framework considered in this paper. Many applications in materials science, such as the calculation of free energies, require the integration of the system over long periods of time. In these applications, it is essential that the time integrator have a good long-time behavior, such as conferred by symplecticity and exact conservation properties.

The velocity Verlet scheme, which is identical to Newmark's method (cf., for example [8]) of structural dynamics, is perhaps the most widely used time-integration scheme in molecular dynamics. The constant time-step velocity Verlet scheme is symplectic-momentum preserving and, therefore, does not conserve energy. As it is often the case with symplectic-momentum preserving methods, it nevertheless has good energy-conservation properties for sufficient small time steps. However, due to the conditional stability of the method, the time-step is constrained by the period of thermal vibrations of the atoms, which renders calculations of equilibrium thermodynamic properties exceedingly costly. The development of integration schemes that alleviate or entirely eliminate the time-step restrictions of explicit integration in molecular dynamics applications is the subject of ongoing research (cf., for example [23, 24]).

We proceed to illustrate the performance of energy-stepping in molecular dynamics applications by analyzing the dynamics of a simple argon cluster. Specifically, we consider the numerical experiment proposed by Biesiadecki and Skeel [25]. The experiment concerns the two-dimensional simulation of a seven-atom argon cluster, six atoms of which are arranged symmetrically around the remaining central atom, Figure 5. The atoms interact via the pairwise Lennard-Jones potential

$$\phi(r) = 4\varepsilon\left[\left(\frac{\sigma}{r}\right)^{12} - \left(\frac{\sigma}{r}\right)^{6}\right] \tag{66}$$

where r is the distance between two atomic centers, $\varepsilon/k_B = 119.8\,\mathrm{K}$ and $\sigma = 0.341\,\mathrm{nm}$ are material constants for Argon, and $k_B = 1.380658 \times 10^{-23}\,\mathrm{J/K}$ is the Boltzmann's constant. In addition, the mass of an argon atom is $m = 66.34 \times 10^{-27}\,\mathrm{kg}$. The initial positions of the atoms are slightly perturbed about the configuration that minimizes the potential energy of the cluster. The initial velocities are chosen such that the total linear momentum is zero and the center of mass of the cluster remains fixed. The corresponding total energy of the cluster is $E/\varepsilon = -10.519$. Table I summarizes the initial conditions for the simulation.

Three different energy steps are employed in the energy-stepping calculations: $h_1 = E_0/100$, $h_2 = E_0/60$ and $h_3 = E_0/30$. The time steps employed in the velocity Verlet calculations are

DOI: 10.1002/nme

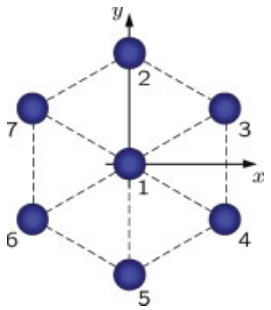

Figure 5. Frozen argon cluster.

Table I. Frozen argon cluster: initial conditions.

Atom	1	2	3	4	5	6	7
Position (nm)	0.00	0.02	0.34	0.36	−0.02	−0.35	−0.31
	0.00	0.39	0.17	−0.21	−0.40	−0.16	0.21
Velocity (nm/nsec)	−30	50	−70	90	80	−40	−80
	−20	−90	−60	40	90	100	−60

$\Delta t_1 = 56.98$ fs, $\Delta t_2 = 87.56$ fs and $\Delta t_3 = 124.88$ fs. These time steps correspond to the average time steps resulting from the respective energy-stepping calculations. The total duration of the analysis is 100 ns.

Figure 6 shows the evolution in time of the total energy. As expected, energy-stepping is energy preserving regardless the energy step employed. By way of sharp contrast, whereas velocity Verlet has remarkable energy behavior for the short time step, it becomes unstable for the intermediate time step and blows up for the larger time step. This blow-up behavior is expected owing to the conditional stability of velocity Verlet.

In order to assess the long-time behavior of energy-stepping, we study the qualitative behavior of the trajectories of the argon atoms for a time window of [99.95,100] ns, corresponding to the last 50 000 fs of the simulations. A velocity Verlet solution computed with a time step equal to $\Delta t = 10$ fs is presumed to be ostensibly converged and is used by way of reference. Trajectories of the seven argon atoms, each represented by a different color, are depicted in Figure 7 and the configuration at $t = 0$ is represented by the dashed line hexagon. A notable feature of the energy-stepping trajectories is that, even for large time steps, they remain stable over long periods of time.

Finally, the convergence statement of Theorem 4.4 is illustrated by Figure 8. We first recall that, as demonstrated in Section 4, the approximate space of trajectories is $X = W^{1,p}(0,T)$, $p<\infty$, and of particular interest is the space $H^1(0,T) := W^{1,2}(0,T)$. Then, distances are measured with respect to the H^1-norm

$$\|q\|_{H^1(0,T)} = \left(\int_0^T (|q(t)|^2 + |\dot{q}(t)|^2)\, \mathrm{d}t \right)^{1/2} \tag{67}$$

DOI: 10.1002/nme

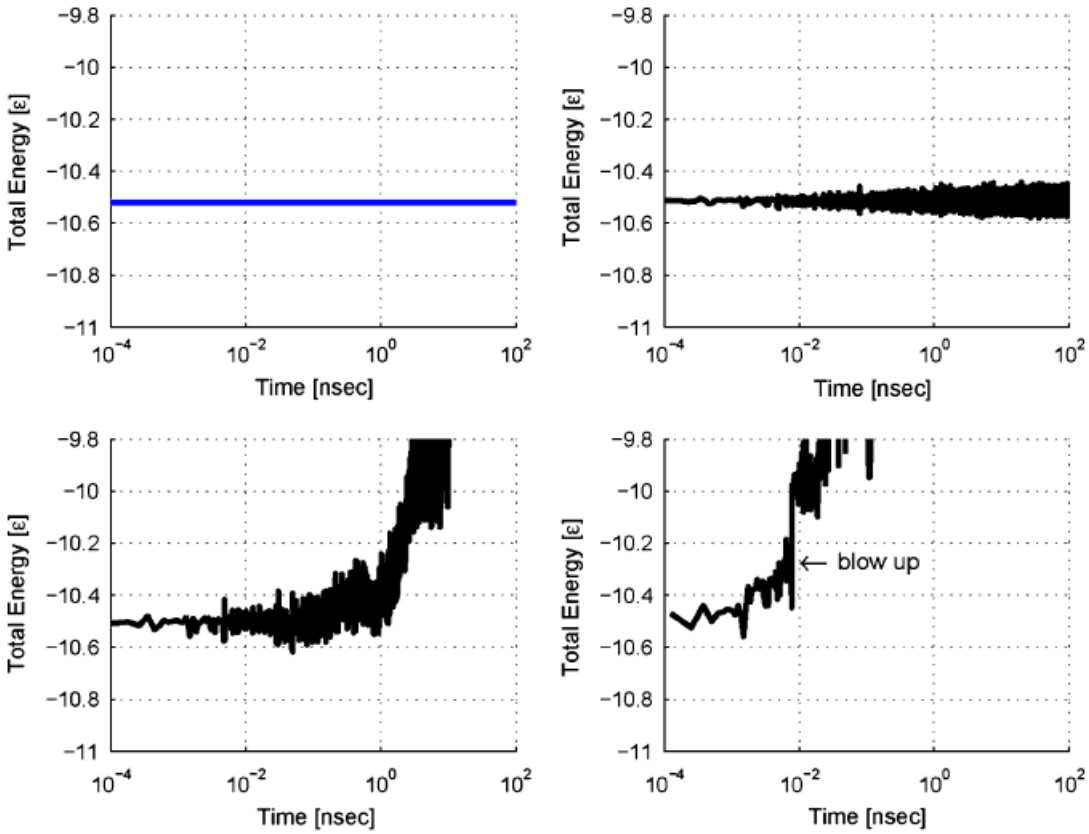

Figure 6. Frozen argon cluster. Top left: Energy-stepping. Top-right: Velocity Verlet, $\Delta t_1 = 56.98\,\text{fs}$. Bottom-left: Velocity Verlet, $\Delta t_2 = 87.56\,\text{fs}$. Bottom-right: Velocity Verlet, $\Delta t_3 = 124.88\,\text{fs}$.

and a relative H^1-error is defined by

$$H^1\text{-error} = \frac{|\|q_h\|_{H^1(0,T)} - \|q\|_{H^1(0,T)}|}{\|q\|_{H^1(0,T)}} \tag{68}$$

where $\|q\|_{H^1(0,T)}$ is estimated from numerical results. The relative H^1-error is shown on the left side of Figure 8 as a function of the energy step, for $T = 1\,\text{ns}$. The slope of the convergence plot is also directly related to the rate of convergence in energy step h, that is $H^1\text{-error} = O(h^r)$. This gives an estimated rate of convergence in the H^1-norm of $r \simeq \frac{1}{2}$. Furthermore, it is interesting to observe on the right side of Figure 8 that the average and the maximum time steps selected by energy-stepping are $O(h)$ and $O(h^{1/2})$, respectively. Therefore, the sequence q_h is indeed convergent, transversal, and $\lim_{h\to 0} \max_i \Delta t_i = 0$, as expected from the discussion in Section 4.3.

5.2. *Finite-element models*

Next we consider the finite-dimensional Lagrangian systems obtained by a finite-element discretization of the action of a nonlinear elastic solid (cf., e.g. [3] for details of finite-element approximation

DOI: 10.1002/nme

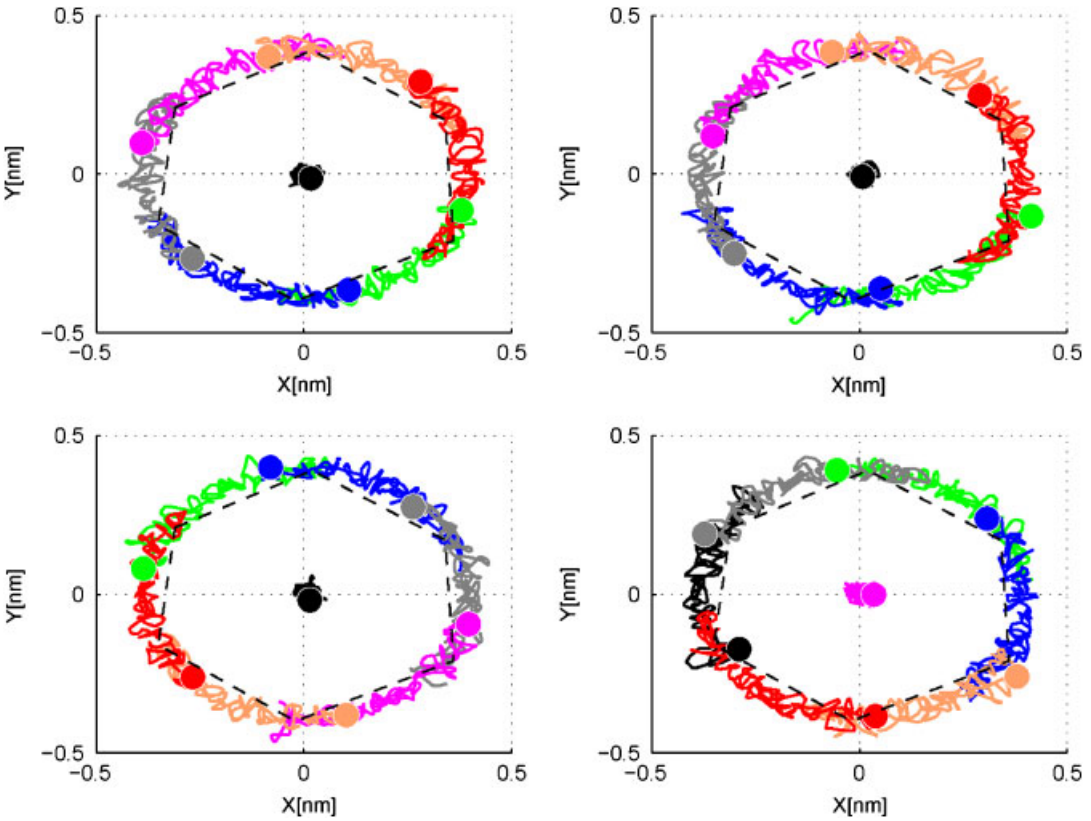

Figure 7. Trajectories of argon atoms for a time window of [99.95,100] ns. The dashed line hexagon represents the initial position of the atoms. Top-left: velocity Verlet, $\Delta t = 10\,\text{fs}$. Top-right: Energy-stepping, $h_1 = E_0/100$. Bottom-left: Energy-stepping, $h_2 = E_0/60$. Bottom-right: Energy-stepping, $h_3 = E_0/30$.

in elastodynamics). For these applications, the generalized coordinates q of the system are the coordinates of the nodes in the deformed configuration of the solid. We present two numerical examples that illustrate the performance of energy-stepping in that area of application. The first example concerns the dynamics of a spinning neo-Hookean cube, the second concerns the collision of two neo-Hookean spheres. In all applications, we assume a strain-energy density of the form

$$W(F) = \frac{\lambda_0}{2}(\log J)^2 - \mu_0 \log J + \frac{\mu_0}{2}\,\text{tr}(F^{\text{T}}F) \tag{69}$$

which describes a neo-Hookean solid extended to the compressible range. In this expression, λ_0 and μ_0 are the Lamé constants.

In problems involving contact we additionally consider the kinematic restrictions imposed by the impenetrability constraint. We recall that the admissible configuration set $\mathscr{C}$ of a deformable body is the set of deformation mappings which are globally one-to-one. In so-called *barrier* methods, the interpenetration constraint may be accounted for by adding the indicator function $I_{\mathscr{C}}(q)$ of the admissible set $\mathscr{C}$ to the energy of the solid. We recall that the indicator function of a set $\mathscr{C}$ is the

DOI: 10.1002/nme

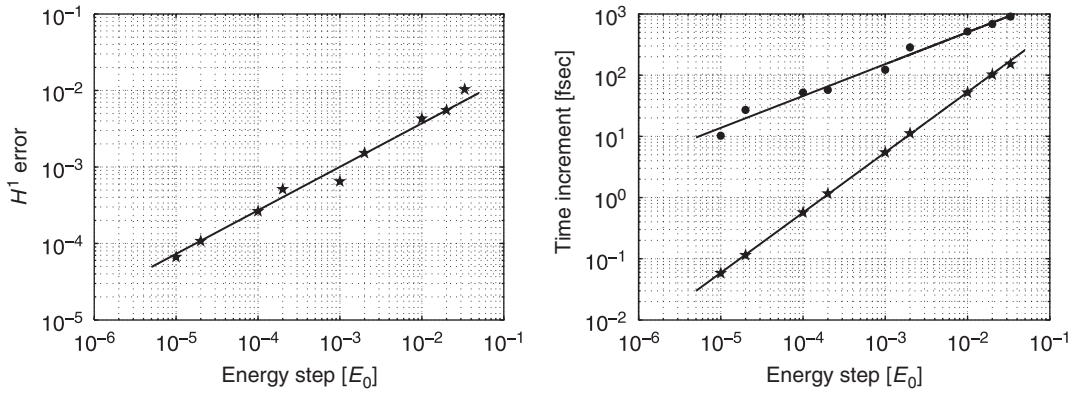

Figure 8. Convergence analysis of the frozen argon cluster. Left: Convergence is observed in the H^1-norm with estimated convergence rate of $r \simeq 1/2$. Right: The average ($\star$) and the maximum ($\bullet$) time steps selected by energy-stepping are $O(h)$ and $O(h^{1/2})$, respectively.

extended-valued function

$$I_{\mathscr{C}}(q) = \begin{cases} 0 & \text{if } q \in \mathscr{C} \\ \infty & \text{otherwise} \end{cases} \tag{70}$$

Kane *et al.* [26] and Pandolfi *et al.* [27] have provided a computationally convenient characterization of the admissible set $\mathscr{C}$ for polyhedra, such as the result from a discretization of the domain $\mathscr{B}$ by simplices, as the set of configurations that are free of intersections between any pair of element faces, Figure 9. Thus, $q \in \mathscr{C}$ if no pair of element faces intersect, $q \notin \mathscr{C}$ otherwise. Often in calculations, the indicator function $I_{\mathscr{C}}$ is replaced by a penalty approximation $I_{\mathscr{C},\varepsilon} \geqslant 0$ parameterized by a small parameter $\varepsilon > 0$ and such that $I_{\mathscr{C},\varepsilon} = 0$ over $\mathscr{C}$. In this approach, as $\varepsilon \to 0$, $I_{\mathscr{C},\varepsilon} \to I_{\mathscr{C}}$ pointwise and interpenetration is increasingly penalized. A convenient choice of penalty energy function for contact is of the form (Kane *et al.* [26] and Pandolfi *et al.* [27])

$$I_{\mathscr{C},\varepsilon}(q) = \frac{1}{2\varepsilon} \sum_{\alpha \in I} g_\alpha(q) \tag{71}$$

where the index set I ranges over all pairs of boundary faces and

$$g_\alpha(q) = \begin{cases} 0 & \text{if the faces do not intersect} \\ \|A - B\|^2 & \text{otherwise} \end{cases} \tag{72}$$

where A and B are the two extreme points of the intersection between a pair of simplices, as shown in Figure 9. It follows from the invariance properties of the admissible set $\mathscr{C}$ that $I_{\mathscr{C}}(q)$ and $I_{\mathscr{C},\varepsilon}(q)$ are themselves invariant under the action of translations and rotations. It therefore follows that the constrained Lagrangian retains its energy and momentum preserving properties.

The application of energy-stepping to dynamical problems subject to set constraints, and in particular to dynamic contact problems, is straightforward. The case in which the constraints are represented by means of a penalty energy function $I_{\mathscr{C},\varepsilon}$ falls right within the general framework and requires no special considerations. In addition, energy-stepping provides an efficient means of

DOI: 10.1002/nme

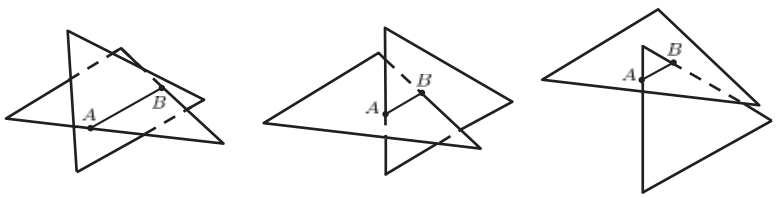

Figure 9. Three types of intersections between boundary simplices.

enforcing set constraints exactly. Thus, suppose that the set constraints are accounted for by the addition of the corresponding indicator function $I_{\mathscr{C}}$ to the energy, as discussed earlier. Then, the boundary $\partial\mathscr{C}$ of the admissible set is an energy step of infinite height that necessarily causes the energy-stepping trajectory to reflect. In this case, the only modification of the algorithm that is required consists of restricting the solution of (27) to the admissible set $\mathscr{C}$. When the admissible set is the intersection of the zero sets of non-negative constraint functions $\{g_\alpha, \alpha \in I\}$, this restriction simply corresponds to choosing t_{i+1} as the minimum of the solution of (27) and of the solutions of

$$g_\alpha(q_i + (t_{i+1} - t_i)\dot{q}_i) = 0^+ \tag{73}$$

In particular, collision is automatically captured by the intrinsic time adaption of energy-stepping (cf., for example [28, 29], for a detailed discussion of time-step selection considerations in contact problems).

For the purposes of assessing the performance of energy-stepping, in the subsequent examples, we draw detailed comparisons with the second-order explicit Newmark method, namely, the member of the Newmark family of time-stepping algorithms corresponding to parameters $\beta = 0$ and $\gamma = \frac{1}{2}$ (cf., for expample [8] for a detailed account of Newmark's method). In the linear regime, explicit Newmark is second-order accurate and conditionally stable, with a critical time step equal to twice over the maximum natural frequency of the system. As already noted, explicit Newmark is identical to velocity Verlet. For constant time step it is also identical to central differences. It can also be shown that the Newmark solution is in one-to-one correspondence, or 'shadows', the solution of the trapezoidal-rule variational integrators (cf., for example [8]). Thus, explicit Newmark provides a convenient representative of a time-integrator commonly used in molecular dynamics, finite-differencing and variational integration.

Detailed analyses of the implicit members of the Newmark family of algorithms, their stability and energy preserving properties (for linear systems) were given in Belytschko and Schoeberle [30], Hughes [12] and related papers.

5.2.1. Spinning neo-Hookean cube. Our next example concerns the spinning of a free-standing elastic cube of unit size. The mesh comprises 12 288 4-node tetrahedral isoparametric elements and 2969 nodes. The cube is a compressible neo-Hookean solid characterized by a strain-energy density of the form (69). The values of the material constants in (69) are: $\lambda_0 = 0.0100$, $\mu_0 = 0.0066$ and $\rho = 0.100$. The cube is imparted an initial angular velocity $\omega_0 = 1$ about one of its axes. The material properties are chosen such that the cube is compliant and undergoes nonlinear dynamics consisting of an overall low-frequency rotation coupled to large-amplitude high-frequency vibrations. A sequence of snapshots of the energy-stepping trajectory corresponding to $h = 10^{-5}$ are shown

DOI: 10.1002/nme

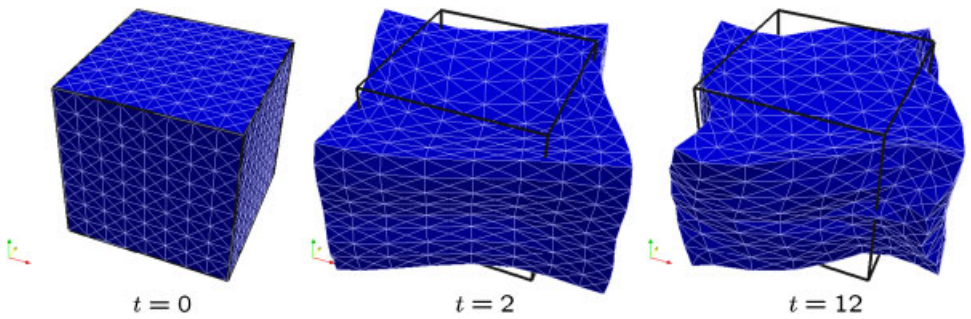

Figure 10. Spinning neo-Hookean cube. Snapshots of the energy-stepping trajectory for $h = 10^{-5}$ at times $t = 2$ and $t = 12$.

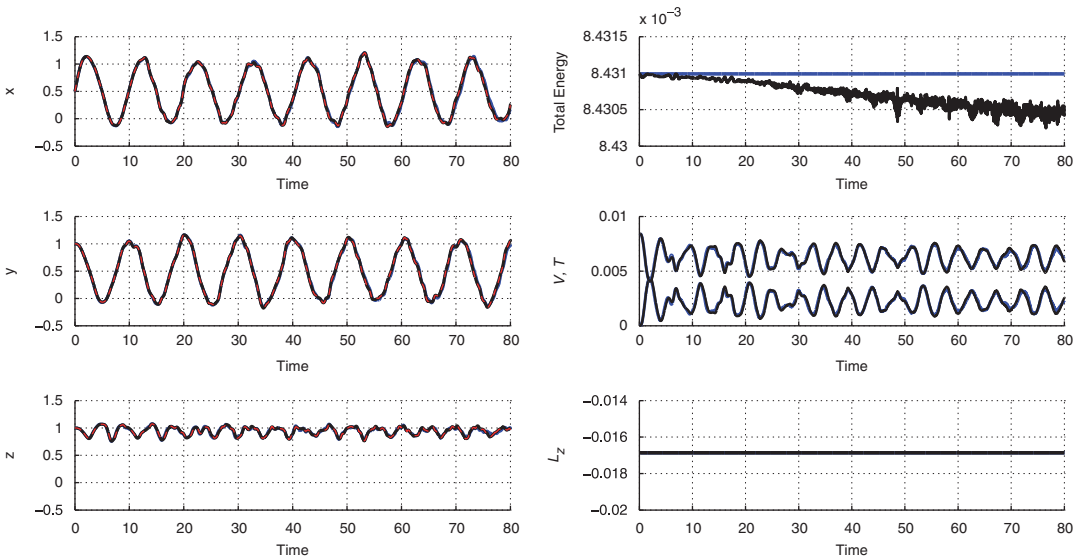

Figure 11. Spinning neo-Hookean cube. Blue line: Energy-stepping solution with $h = 10^{-5}$. Black line: Newmark solution with $\Delta t = 0.0082$. Red line: Newmark solution with $\Delta t = 0.0001$.

on the left side of Figure 10. The large-amplitude oscillations undergone by the spinning cube are evident in the figure.

The motion of the point $X = (0.5, 1.0, 1.0)$, the total energy, the potential energy, the kinetic energy and the z-component of the total angular momentum are shown in Figures 11–13 for the energy-stepping solutions corresponding to $h = 1 \times 10^{-5}$, $h = 3 \times 10^{-5}$ and $h = 6 \times 10^{-5}$, respectively, and for Newmark solutions with $\Delta t = 0.0082$, $\Delta t = 0.0204$ and $\Delta t = 0.0381$, respectively. In every case, the time step employed in the Newmark calculations is the average time step of the corresponding energy-stepping trajectory. In Figure 11, an ostensibly converged Newmark solution computed with a time step of $\Delta t = 0.0001$ is also shown for comparison.

DOI: 10.1002/nme

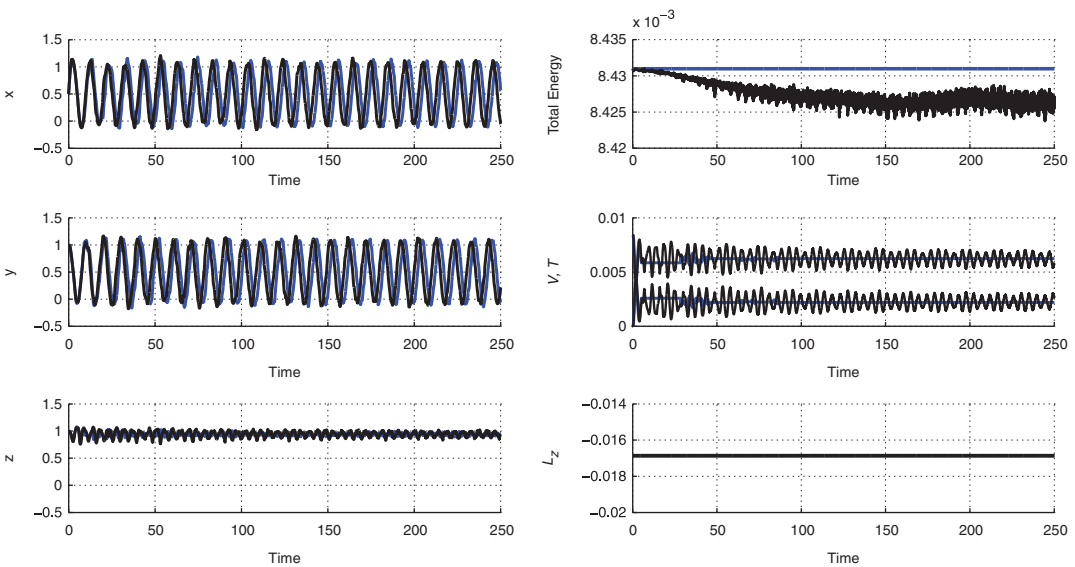

Figure 12. Spinning neo-Hookean cube. Blue line: Energy-stepping solution with $h = 3 \times 10^{-5}$. Black line: Newmark solution with $\Delta t = 0.0204$.

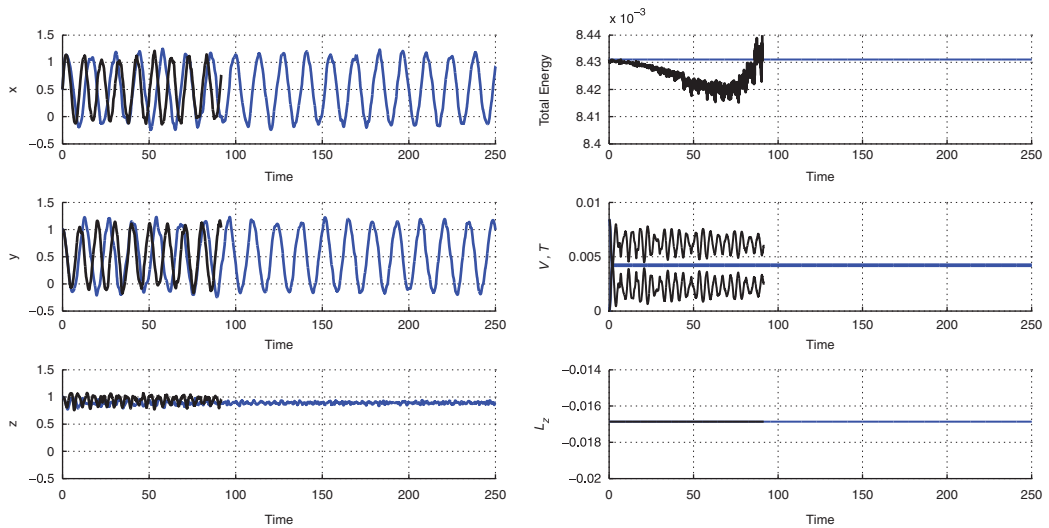

Figure 13. Spinning neo-Hookean cube. Blue line: Energy-stepping solution with $h = 6 \times 10^{-5}$. Black line: Newmark solution with $\Delta t = 0.0381$.

For the smaller energy and time steps, both the energy-stepping and Newmark solutions are ostensibly converged up to a time of 80. It bears emphasis that no special precautions are taken to ensure transversality of the energy-stepping trajectory, as defined in Definition 4.1, which provides an indication that non transversality is a rare event that is unlikely to turn up in practice.

DOI: 10.1002/nme

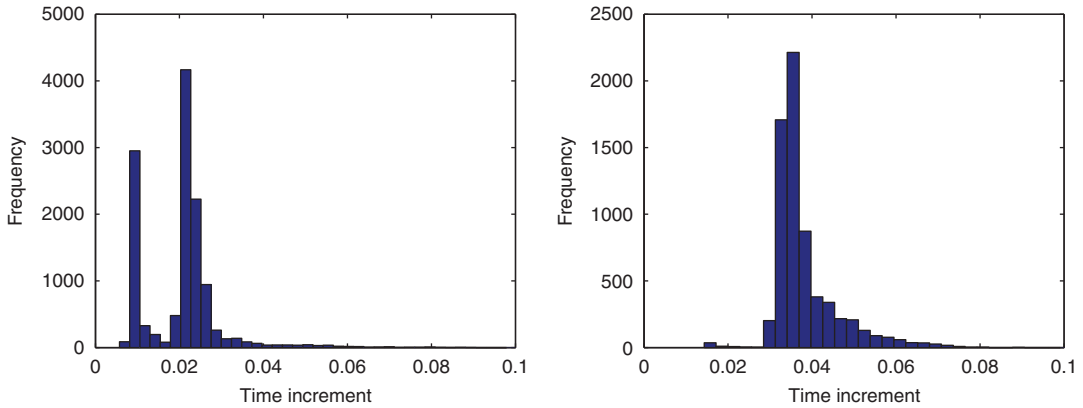

Figure 14. Spinning neo-Hookean cube. Histogram of time steps selected by energy-stepping. Left: $h=3\times10^{-5}$. Right: $h=6\times10^{-5}$.

As expected, both solutions additionally exhibit exact linear and angular momentum conversation. In addition, the energy-stepping solution also exhibits exact energy conservation. By contrast, in Newmark's solution the total energy, while bounded, drifts somewhat. These trends are accentuated at the intermediate energy and time steps. By way of sharp contrast, at the larger energy and time steps, the stability, energy and momentum conservation properties of energy-stepping are maintained, while the Newmark solution loses stability and blows up.

Finally, Figure 14 shows a histogram of the time steps selected by energy-stepping for the intermediate and the largest energy steps. The broad range of time steps is noteworthy, as is the scaling of the average time step with the energy step employed in the calculation. Thus, a small (large) energy step results in comparatively smaller (larger) time steps on average, as expected. Figure 14 also illustrates the automatic time-selection property of energy-stepping. This property may in turn be regarded as the means by which energy-stepping achieves symplecticity and exact energy conservation. It also bears emphasis that, unlike variable time-step variational integrators designed to conserve energy [2, 3], energy-stepping always selects a valid (albeit possibly infinite) time step and is therefore free of solvability concerns.

5.2.2. Dynamic contact of two neo-Hookean spherical balls. Our last example concerns the collision of two free-standing elastic balls of unit radius, Figure 15. The mesh of each ball comprises 864 4-node tetrahedral isoparametric elements and 250 nodes. The cube is a compressible neo-Hookean solid characterized by a strain-energy density of the form (69). Initially, one of the balls is stationary, whereas the other ball is imparted an initial head-on velocity of magnitude 5 and and angular velocity of magnitude $\omega_0=2.5$ about an axis perpendicular to the relative position vector between the centers of the balls. The values of the material constants in (69) are $\lambda_0=1.154\times10^8$, $\mu_0=7.96\times10^7$, and $\rho=7800$. As in the preceding example, the material properties are chosen such that the balls are compliant and undergo nonlinear dynamics consisting of an overall rigid-body motion coupled to large-amplitude high-frequency vibrations. The contact constraint is enforced using the penalty energy (71) and (72) with $\varepsilon=10^{-7}$.

Figure 16 compares the time histories of total energy, potential energy, kinetic energy, and time step attendant to the energy-stepping trajectory for $h=10^3$ and Newmark's trajectory for

DOI: 10.1002/nme

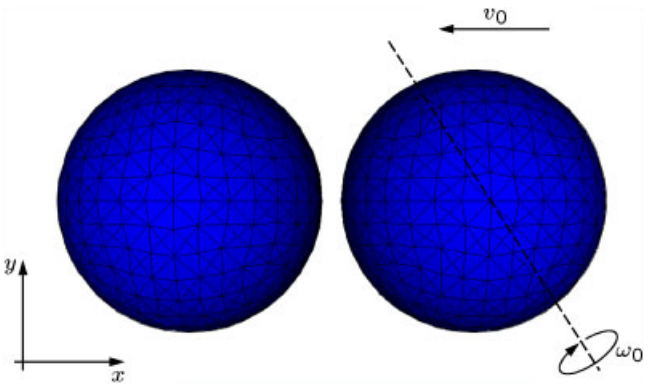

Figure 15. Collision of two neo-Hookean spherical balls.

$\Delta t = 3 \times 10^{-5}$, the latter chosen to be within the range of stability of the Newmark method. As expected, the kinetic energy of the system is partly converted to potential energy during the approach part of the collision sequence, and viceversa during the release part. We recall that period elongation, causing solutions to lag in time is indeed a principal measure of the loss of accuracy of Newmark's method with increasing time step (cf., for example [12]). In this regard it is interesting to note that, despite the selection of a time step much smaller than the average energy-stepping time step, the Newmark kinetic and potential energies lag behind the corresponding energy-stepping energies. Also characteristically, energy-stepping is observed to conserve energy exactly through the collision, whereas the Newmark energy history, while bounded, drifts somewhat. Other notable features of the calculations are the ability of energy-stepping to detect the time of collision (~ 0.1) and to automatically modulate the time step so as to resolve the fine structure of the intricate interactions that occur through the collision.

Figure 17 shows the time history of the center-of-mass linear and angular velocities of each of the balls and of the entire system. The center-of-mass linear and angular velocities of a system are defined as the total linear and angular momenta divided by the total mass, respectively. Because the system is free of external forces, the total linear and angular momentum of the system is conserved through the collision. We note from Figure 17 that the energy-stepping trajectory does indeed conserve total linear and angular momentum exactly. We also note that the transfer of linear momentum from incoming to target ball is largely in the direction of impact, with slight amounts of transfer of linear momentum in the transverse direction and of angular momentum owing to asymmetries in the mesh.

It is interesting to compare the results of the finite-element calculations with the classical theories of impact between smooth rigid bodies (see, for example Reference [31]) and of Hertzian contact between elastic bodies. For two rigid spheres undergoing head-on impact, with the target sphere initially stationary and the incoming sphere having initial speed v_0 and angular velocity ω_0, a conventional way of expressing the final linear and angular velocities is in terms of the coefficient of restitution e. For two spheres of the same mass one has

$$\frac{T_f}{T_0} = \frac{1}{2}(1+e^2) \tag{74}$$

DOI: 10.1002/nme

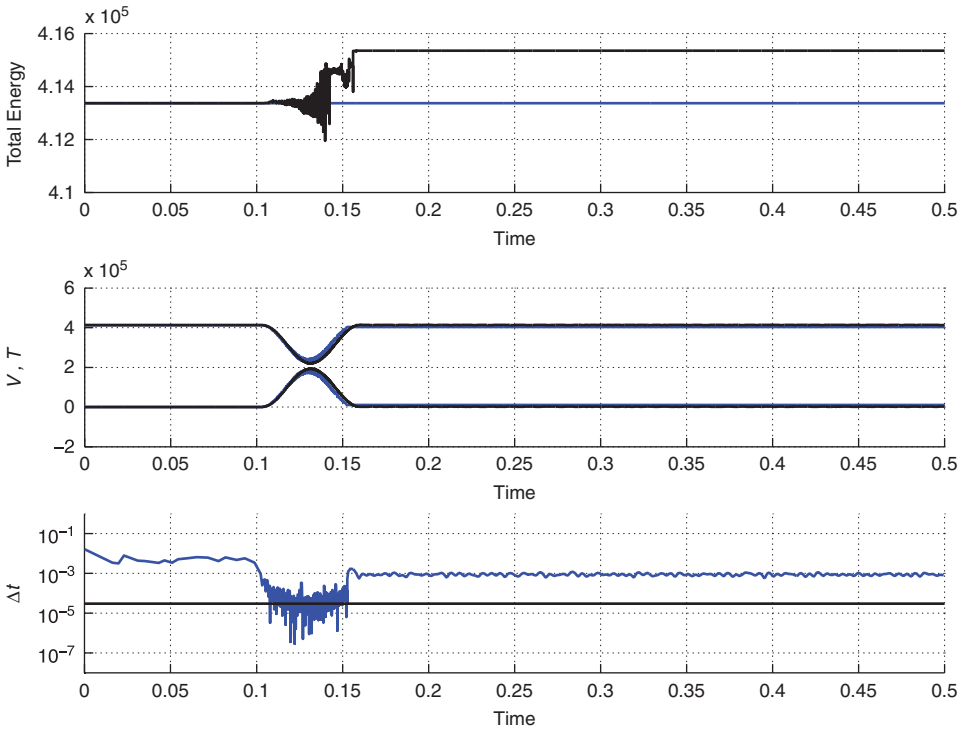

Figure 16. Collision of two neo-Hookean spherical balls. Blue line: Energy-stepping solution with $h=10^3$. Black line: Newmark solution with $\Delta t=3\times10^{-5}$.

where T_0 and T_f are the initial and final kinetic energies of the center-of-mass motion. For the energy-stepping trajectory the final center-of-mass velocities of the balls are

$$V_{1,f}=(-4.91,0.31,0.35),\quad \Omega_{1,f}=(0.001,0.067,-0.044)$$
$$V_{2,f}=(-0.09,-0.31,-0.35),\quad \Omega_{2,f}=(-0.001,1.005,0.044)$$

which roughly correspond to a coefficient of restitution of $e=0.964$. For elastic collisions, the coefficient of restitution provides a simple measure of the fraction of translational kinetic energy that is transferred into vibrational energy along a specific trajectory. We note, however, the coefficient of restitution is not constant but varies from trajectory to trajectory.

Another useful reference point is provided by the Hertzian theory of elastic contact (cf., e.g. [31]). While the theory applies to bodies in static equilibrium only, the resulting laws of interaction are often used to describe the dynamics of systems of spheres [31]. When applied in this manner, the theory predicts a contact duration time

$$\tau=4.53\left[\frac{1-\nu^2}{E}\frac{4}{3}R^3\rho\right]^{2/5}\left[\frac{2}{v_0R}\right]^{1/5} \tag{75}$$

DOI: 10.1002/nme

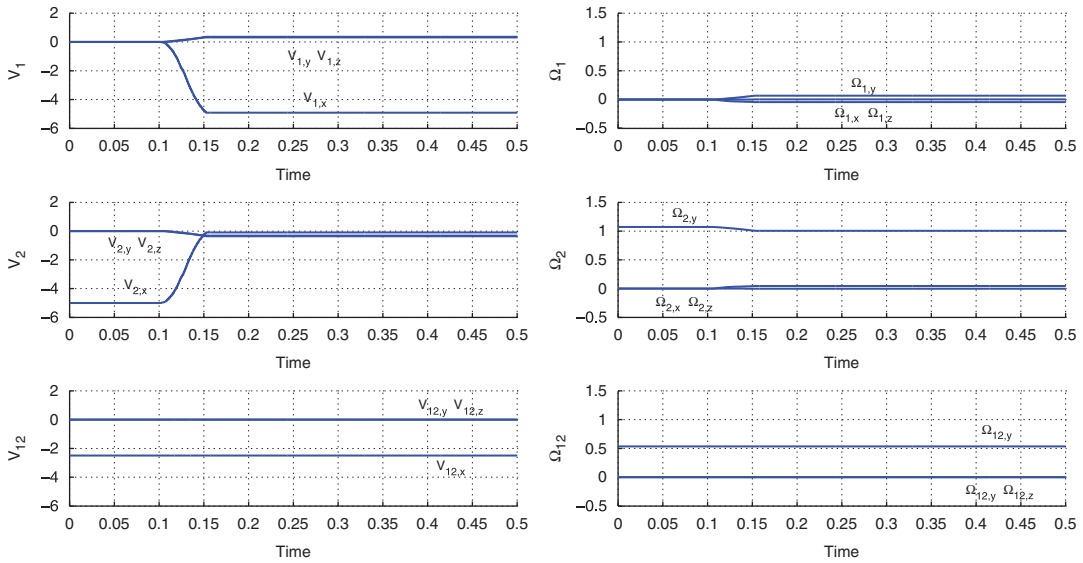

Figure 17. Collision of two neo-Hookean spherical balls. Energy-stepping solution with $h = 10^3$.

where E is Young's modulus, ν Poisson's ratio, ρ is the mass density, R is the radius of the spheres and v_0 is the impact velocity. For the problem under consideration, this formula gives $\tau = 0.069$, whereas the value computed from the energy-stepping solution is $\tau = 0.0476$. Thus, while the Hertzian theory does provide a rough estimate of the contact time, an accurate interpretation of experiments may require more detailed analyses such as presented here.

6. SUMMARY AND DISCUSSION

We have formulated a new class of time-integration schemes for Lagrangian mechanics, which we refer to as *energy-stepping*, that are momentum and energy conserving, symplectic and convergent. In order to achieve these properties we adopt a strategy that may be viewed as the reverse of backward-error analysis. Thus, whereas backward-error analysis seeks to identify a nearby Lagrangian system that is solved exactly by the solutions generated by a numerical integrator, the approach followed here is to directly replace the system by a nearby one that can be solved exactly. We have specifically investigated piecewise-constant approximations of the potential energy obtained by replacing the original potential energy by a stepwise or *terraced* approximation at steps of uniform height. By taking the steps of diminishing height, an approximating sequence of energies is generated. The trajectories of the resulting approximating Lagrangians can be characterized explicitly and consist of intervals of piecewise rectilinear motion. We have shown that the energy-stepping trajectories are symplectic, exactly conserve all the momentum maps of the original system and, subject to a transversality condition, converge to trajectories of the original system when the energy step is decreased to zero. These properties are born out by selected examples of application, including the dynamics of a frozen Argon cluster, the spinning of an elastic cube and

DOI: 10.1002/nme

the collision of two elastic spheres. These examples additionally showcase the excellent long-term behavior of energy-stepping, its automatic time-step selection property, and the ease with which it deals with systems with constraints, including contact problems.

It is suggestive to note that in classical Hamiltonian mechanics energy and time are conjugate variables. Conventional integration schemes are based on discretizing time, and the energy history then follows as a corollary to the integration scheme. By contract, energy-stepping may be regarded as the result of discretizing energy, with the time increments then following from the integration scheme. In this manner, energy-stepping schemes may be regarded as *dual* to time-stepping schemes.

We close by pointing out some limitations of our analysis and possible avenues for extensions of the approach.

First, our convergence analysis relies on a technical condition of transversality of the energy-stepping trajectory. It is possible that such a transversality condition can be relaxed if slight adjustments of the initial conditions are allowed and by assuming suitable lower bounds on the curvature of the energy surface. Indeed, our experience with selected numerical tests appears to indicate that the transversality condition is not of major concern in practice. However, a more clear delineation of essential and inessential conditions for the convergence of energy-stepping is desirable, if beyond the scope of this paper.

Second, it is clear that a piecewise-constant energy approximation of the potential energy is not the only—perhaps even the best—approximation that generates exactly solvable Lagrangians. A case in point consists of piecewise linear approximations of the potential energy over a simplicial grid. The corresponding approximating trajectories are piecewise parabolic and corresponds to *free fall* within each of the simplices of the energy grid. As the corresponding force field is piecewise constant the time-integration scheme thus defined may be thought of as *force-stepping*. The convergence properties of force-stepping are in fact much more readily established that those of energy stepping. However, a drawback of force stepping is that the approximating Lagrangian necessarily breaks some of the symmetries of the original Lagrangian in general. The systematic investigation of approximation schemes of the type proposed here, the elucidation of their properties and the determination of the best types of approximating Lagrangians in each area of application, are worthwhile directions of future research.

APPENDIX: VERIFICATION OF THE SYMPLECTICITY OF THE ENERGY-STEPPING SCHEME

We proceed to verify that the identities (41) are identically satisfied by the energy-stepping scheme. For simplicity of notation and without loss of generality we take the mass matrix to be of the form $M=mI$. In addition, it suffices to consider mappings defined by the trajectory depicted in Figure 2, the general result then following by recursion. Evidently, the symplectic form is trivially conserved for $t\in[t_0,t_1)$, where t_1 is the time of intersection with the potential energy jump. For $t\in(t_1,t_2)$, the dependence of t_1 on the initial conditions $(\dot{q}_0,q_0)$ must be carefully accounted for. The follow relations are readily computed:

$$\frac{\partial t_1}{\partial \dot{q}_0}=(t_1-t_0)\frac{\partial t_1}{\partial q_0}=-\frac{t_1-t_0}{\dot{q}_0\cdot n_1}n_1=-\left|\frac{\partial t_1}{\partial \dot{q}_0}\right|n_1$$

DOI: 10.1002/nme

$$\frac{\partial n_1}{\partial \dot{q}_0} = (t_1 - t_0)\frac{\partial n_1}{\partial q_0}$$

$$\frac{\partial n_1}{\partial q_0} = \frac{D^2 V_1}{\|\nabla V_1\|} - \frac{n_1 \otimes n_1 \cdot D^2 V_1}{\|\nabla V_1\|} - \frac{D^2 V_1 \cdot \dot{q}_0 \otimes n_1}{\|\nabla V_1\|(\dot{q}_0 \cdot n_1)} + \frac{(n_1 \cdot D^2 V_1 \cdot \dot{q}_0) n_1 \otimes n_1}{\|\nabla V_1\|(\dot{q}_0 \cdot n_1)}$$

For $t \in (t_1, t_2)$ we have

$$\dot{q}(q_0, \dot{q}_0, t) = \dot{q}_0 + \lambda_1 n_1$$

$$q(q_0, \dot{q}_0, t) = q_0 + (t - t_0)\dot{q}_0 + (t - t_1)\lambda_1 n_1$$

where

$$\lambda_1 = \lambda_1(q_0, \dot{q}_0) = -\dot{q}_0 \cdot n_1 + \text{sign}(\Delta V)\sqrt{(\dot{q}_0 \cdot n_1)^2 - \frac{2\Delta V}{m}}$$

and

$$\frac{\partial \lambda_1}{\partial \dot{q}_0} = \frac{-\lambda_1}{\dot{q}_0 \cdot n_1 + \Delta \dot{q}} n_1 + (t_1 - t_0)\frac{\partial \lambda_1}{\partial q_0}$$

$$\frac{\partial \lambda_1}{\partial q_0} = -\frac{\lambda_1}{\|\nabla V_1\|(\dot{q}_0 \cdot n_1 + \lambda_1)} \dot{q}_0 \cdot D^2 V_1 + \frac{\lambda_1(\dot{q}_0 \cdot n_1)}{\|\nabla V_1\|(\dot{q}_0 \cdot n_1 + \lambda_1)} n_1 \cdot D^2 V_1$$
$$+ \frac{\lambda_1(\dot{q}_0 \cdot D^2 V_1 \cdot \dot{q}_0) - \lambda_1(n_1 \cdot D^2 V_1 \cdot \dot{q}_0)(\dot{q}_0 \cdot n_1)}{(\dot{q}_0 \cdot n_1 + \lambda_1)\|\nabla V_1\|(\dot{q}_0 \cdot n_1)} n_1$$

From these identities, the components of the Jacobian matrix $T\varphi$ are found to be

$$P_q = \frac{\lambda_1}{\|\nabla V_1\|} D^2 V_1 - \frac{\lambda_1 \lambda_1}{\|\nabla V_1\|(\dot{q}_0 \cdot n_1 + \lambda_1)} n_1 \otimes n_1 \cdot D^2 V_1 - \frac{\lambda_1}{\|\nabla V_1\|(\dot{q}_0 \cdot n_1 + \lambda_1)} n_1 \otimes \dot{q}_0 \cdot D^2 V_1$$
$$- \frac{\lambda_1}{\|\nabla V_1\|(\dot{q}_0 \cdot n_1)} D^2 V_1 \cdot \dot{q}_0 \otimes n_1 + \frac{\lambda_1(\dot{q}_0 + \lambda_1 n_1) \cdot (D^2 V_1 \cdot \dot{q}_0)}{(\dot{q}_0 \cdot n_1 + \lambda_1)\|\nabla V_1\|(\dot{q}_0 \cdot n_1)} n_1 \otimes n_1$$

$$Q_q = (t - t_1) P_q + \left[I + \frac{\lambda_1}{\dot{q}_0 \cdot n_1} n_1 \otimes n_1 \right]$$

$$P_p = I - \frac{\lambda_1}{(\dot{q}_0 \cdot n_1 + \lambda_1)} n_1 \otimes n_1 + (t_1 - t_0) P_q$$

$$Q_p = (t - t_1) P_p + (t_1 - t_0)\left[I + \frac{\lambda_1}{\dot{q}_0 \cdot n_1} n_1 \otimes n_1 \right]$$

In addition,

$$P_p^{\mathrm{T}} Q_p = (t - t_1) P_p^{\mathrm{T}} P_p + (t_1 - t_0) I + (t_1 - t_0)^2 P_q^{\mathrm{T}} \cdot \left[I + \frac{\lambda_1}{\dot{q}_0 \cdot n_1} n_1 \otimes n_1 \right] = \text{sym}$$

$$Q_q^{\mathrm{T}} P_q = (t - t_1) P_q^{\mathrm{T}} P_q + \left[I + \frac{\lambda_1}{\dot{q}_0 \cdot n_1} n_1 \otimes n_1 \right] \cdot P_q = \text{sym}$$

DOI: 10.1002/nme

$$P_p^{\mathrm{T}} Q_q = Q_p^{\mathrm{T}} P_q + I = I + (t-t_1)\left[I - \frac{\lambda_1}{\dot{q}_0 \cdot n_1 + \lambda_1} n_1 \otimes n_1\right] \cdot P_q$$

$$+ (t_1 - t_0)(t-t_1) P_q^{\mathrm{T}} P_q + (t_1 - t_0) P_q^{\mathrm{T}} \cdot \left[I + \frac{\lambda_1}{\dot{q}_0 \cdot n_1} n_1 \otimes n_1\right]$$

and the symplecticity relations (41) follow from the identity

$$\left[I + \frac{\lambda_1}{\dot{q}_0 \cdot n_1} n_1 \otimes n_1\right] \cdot P_q = \mathrm{sym} = \frac{\lambda_1}{\|\nabla V_1\|} D^2 V_1 + \frac{\lambda_1 (\dot{q}_0 \cdot D^2 V_1 \cdot \dot{q}_0)}{\|\nabla V_1\| (\dot{q}_0 \cdot n_1)^2} n_1 \otimes n_1$$

$$- \frac{\lambda_1}{\|\nabla V_1\| (\dot{q}_0 \cdot n_1)} [D^2 V_1 \cdot \dot{q}_0 \otimes n_1 + n_1 \otimes \dot{q}_0 \cdot D^2 V_1]$$

The symplecticity of the energy-stepping scheme is thus directly verified.

ACKNOWLEDGEMENTS

The authors gratefully acknowledge the support of the US Department of Energy through Caltech's PSAAP Center for the Predictive Modeling and Simulation of High-Energy Density Dynamic Response of Materials.

REFERENCES

1. Ge Z, Marsden JE. Lie–Poisson integrators and Lie–Poisson Hamilton–Jacobi theory. *Physics Letters A* 1988; **133**(3):134–139.
2. Kane C, Marsden JE, Ortiz M. Symplectic energy-momentum preserving variational integrators. *Journal of Mathematical Physics* 1999; **40**(7):3353–3371.
3. Lew A, Marsden JE, Ortiz M, West M. Asynchronous variational integrators. *Archive for Rational Mechanics and Analysis* 2003; **167**:85–146.
4. Marsden JE, West M. Discrete mechanics and variational integrators. *Acta Numerica* 2001; **10**:357–514.
5. Lew A, Marsden JE, Ortiz M, West M. An overview of variational integrators. *Finite Element Methods*: *1970's and Beyond*. CIMNE: Barcelona, 2003.
6. Lew A, Marsden JE, Ortiz M, West M. Variational time integrators. *International Journal for Numerical Methods in Engineering* 2004; **60**(1):151–212.
7. Hairer E, Lubich C, Wanner G. Geometric numerical integration. *Structure-Preserving Algorithms for Ordinary Differential Equations*. Springer Series in Computational Mathematics (2nd edn), vol. 31. Springer: Berlin, 2006.
8. Kane C, Marsden JE, Ortiz M, West M. Variational integrators and the Newmark algorithm for conservative and dissipative mechanical systems. *International Journal for Numerical Methods in Engineering* 2000; **49**(10): 1295–1325.
9. Calvo MP, Sanz-Serna JM. The development of variable-step symplectic integrators, with applications to the two-body problem. *SIAM Journal on Scientific Computing* 1993; **4**:936–952.
10. Gladman B, Duncan M, Candy J. Symplectic integrators for long-term integrations in celestial mechanics. *Celestial Mechanics and Dynamical Astronomy* 1991; **52**:221–240.
11. Bathe K-J. *Finite Element Procedures*. Prentice-Hall: Englewood Cliffs, NJ, 1996.
12. Hughes TJR. *The Finite Element Method*: *Linear Static and Dynamic Finite Element Analysis*. Prentice-Hall: Englewood Cliffs, NJ, 1997.
13. Zienkiewicz OC, Taylor RL. *The Finite Element Method* (5th edn). Butterworth-Heinemann: Stonehamm, MA, 2000.
14. Hairer E, Lubich C. The life-span of backward error analysis for numerical integrators. *Numerische Mathematik* 1997; **76**:441–462.

DOI: 10.1002/nme

15. Reich S. Backward error analysis for numerical integrators. *SIAM Journal on Numerical Analysis* 1999; **36**: 1549–1570.
16. Müller S, Ortiz M. On the Γ-convergence of discrete dynamics and variational integrators. *Journal of Nonlinear Science* 2004; **14**:279–296.
17. Marsden JE, Ratiu TS. *Introduction to Mechanics and Symmetry* (2nd edn). Springer: New York, 1999.
18. Arnold VI. Mathematical methods of classical mechanics. *Graduate Texts in Mathematics* (2nd edn), vol. 60. Springer: New York, 1980.
19. Abraham R, Marsden JE. *Foundations of Mechanics* (2nd edn). Addison-Wesley Publishing Company Inc.: Redwood City, CA., 1987.
20. Hofer H, Zehnder E. Symplectic invariants and Hamiltonian dynamics. *Birkhäuser Advanced Texts*. Birkhäuser: Basel, 1994.
21. Whitney H. *Geometric Integration Theory*. Princeton University Press: Princeton NJ, 1957.
22. Gol'dshtein V, Dubrovskiy S. Lemma Poincaré for $L_{\infty,\mathrm{loc}}$-forms, 2007. arXiv:0712.1682v1. http://arxiv.org/abs/0712.1682x6.
23. Izaguirre JA, Reich S, Skeel RD. Longer time steps for molecular dynamics. *Journal of Chemical Physics* 1999; **110**(20):9853–9864.
24. Humphreys DD, Friesner RA, Berne BJ. A multiple-time step molecular dynamics algorithm for macromolecules. *Journal of Chemical Physics* 1994; **98**(27):6885–6892.
25. Biesiadecki JJ, Skeel RD. Dangers of multiple time step methods. *Journal of Computational Physics* 1993; **109**:318–328.
26. Kane C, Repetto EA, Ortiz M, Marsden JE. Finite element analysis of nonsmooth contact. *Computer Methods in Applied Mechanics and Engineering* 1999; **180**(1–2):1–26.
27. Pandolfi A, Kane C, Marsden JE, Ortiz M. Time-discretized variational formulation of non-smooth frictional contact. *International Journal for Numerical Methods in Engineering* 2002; **53**(8):1801–1829.
28. Carpenter NJ, Taylor RL, Katona MG. Lagrange constraints for transient finite-element surface-contact. *International Journal for Numerical Methods in Engineering* 1991; **32**(1):103–128.
29. Wriggers P. *Computational Contact Mechanics*. Wiley: New York, 2002.
30. Belytschko T, Schoeberle D. On the unconditional stability of an implicit algorithm for nonlinear structural dynamics. *Journal of Applied Mechanics* 1975; **42**:865–869.
31. Goldsmith W. *Impact*: *The Theory and Physical Behaviour of Colliding Solids*. Edward Arnold Ltd.: London, 1960.

DOI: 10.1002/nme